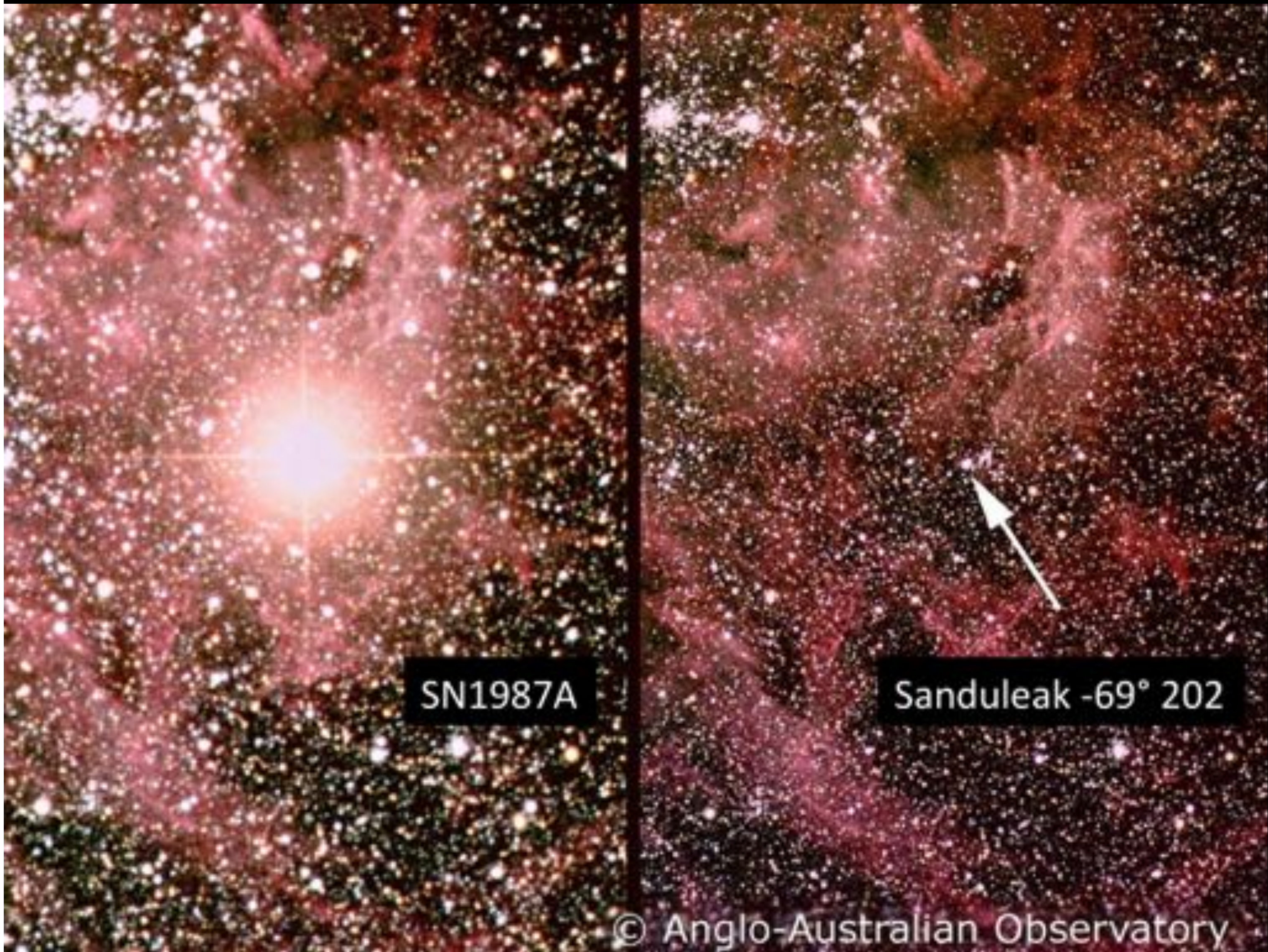

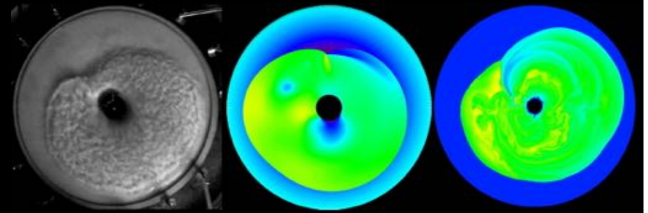

5 lectures on

The Physics of Core-Collapse Supernovae

Outline of lecture 5

Impact on the explosion & new ideas

- Two paths to explosion & signatures
- 2D-3D debate
- Rotation effects: from SASI to low T/W
- Magnetic effects: magnetic SASI, MRI

Progress of ab initio simulations: understandable diversity

-axisymmetric explosions
from first principles
8.1, 9.6 ,11.2, 15, 27M_{sol} (MPA)
12, 15, 20, 25 M_{sol} (ORNL)
(Müller+12a,b,+13, Bruenn+13,+16)

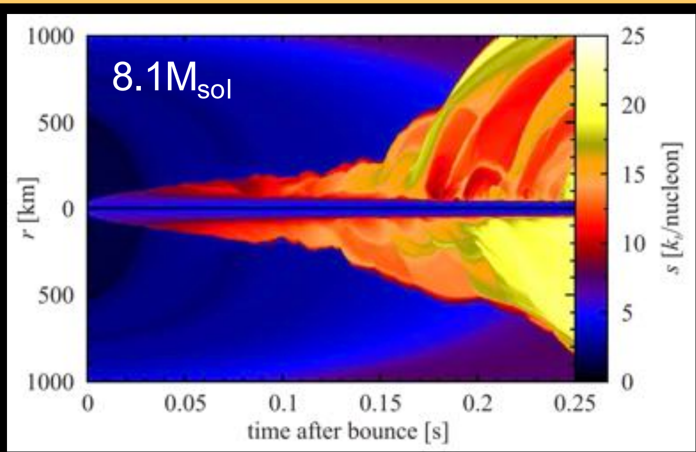

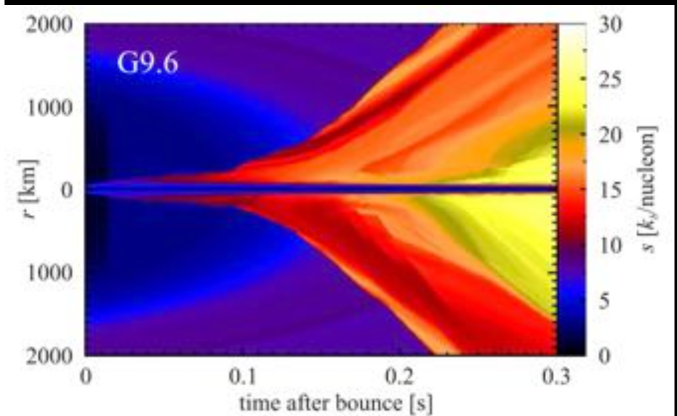

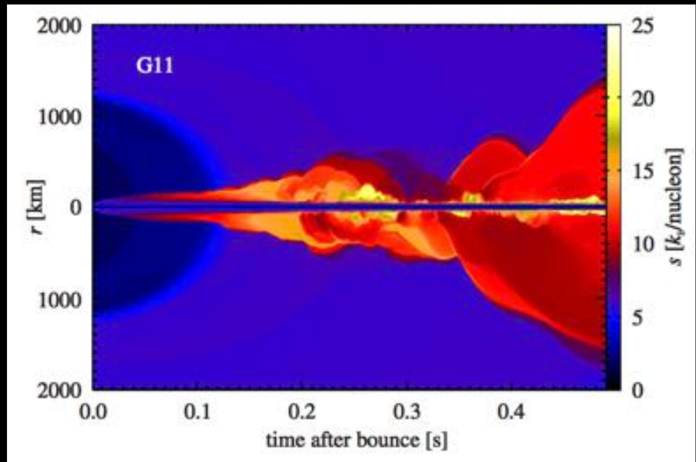

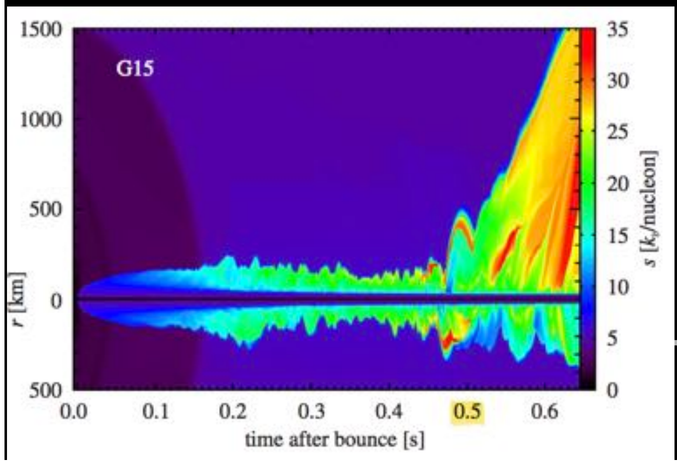

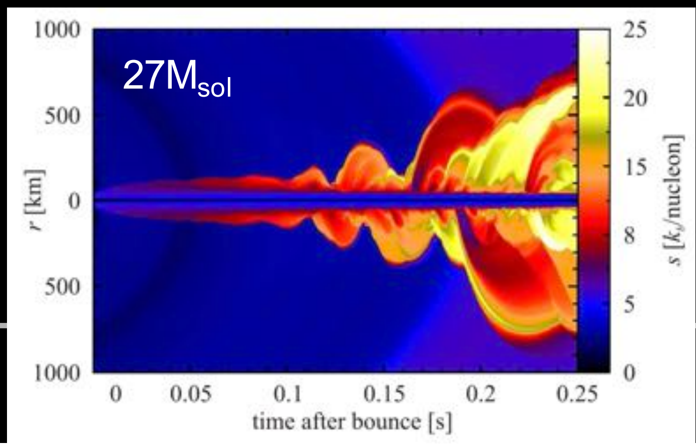

-depending on the progenitor, the dynamical evolution can be dominated by neutrino driven buoyancy (11.2M_{sol}) or by SASI (27M_{sol}) or by both (15M_{sol})

-competition between advection and buoyancy
(Foglizzo+06, Fernandez+13)

$$\chi \equiv \int_{\rm sh}^{\rm gain} \omega_{\rm BV} \frac{{\rm d}r}{v_r} < 3$$

Two paths to explosion (Müller+12)

strength of ν-driven buoyancy:
parameter $\chi \sim \tau_{adv}/\tau_{buoy}$

strength of SASI: amplification parameter Q

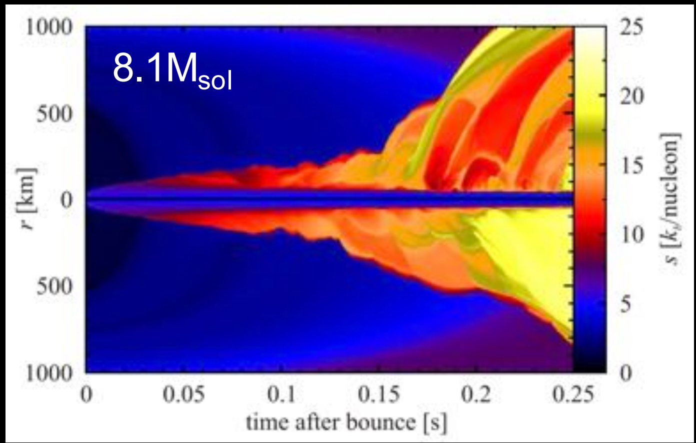

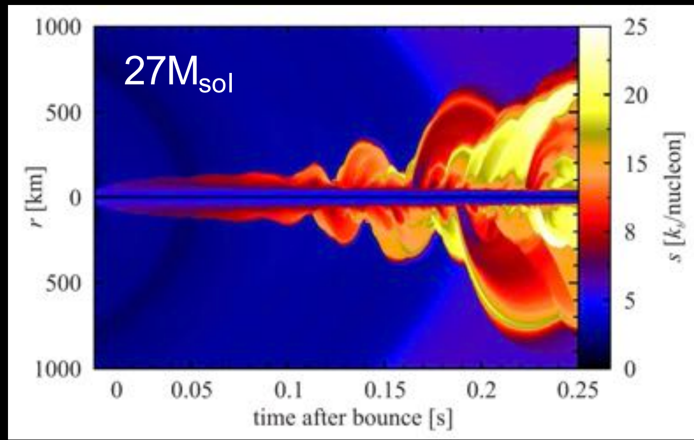

$$\omega_i^{SASI} \equiv \frac{\log Q}{\tau_Q}$$

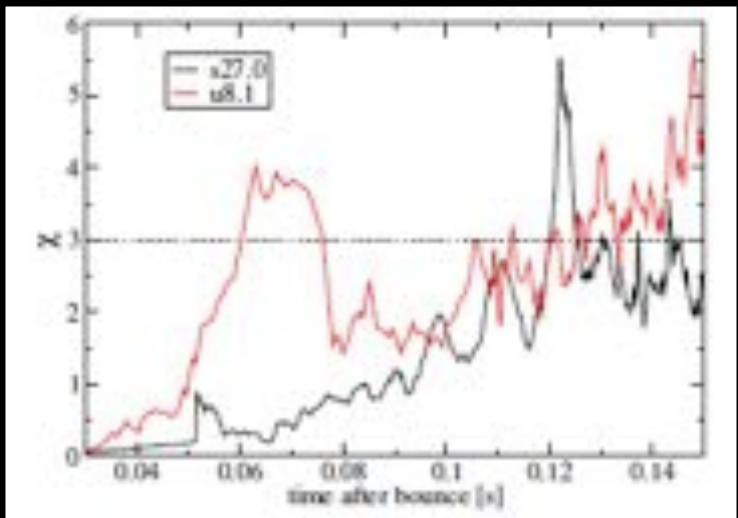

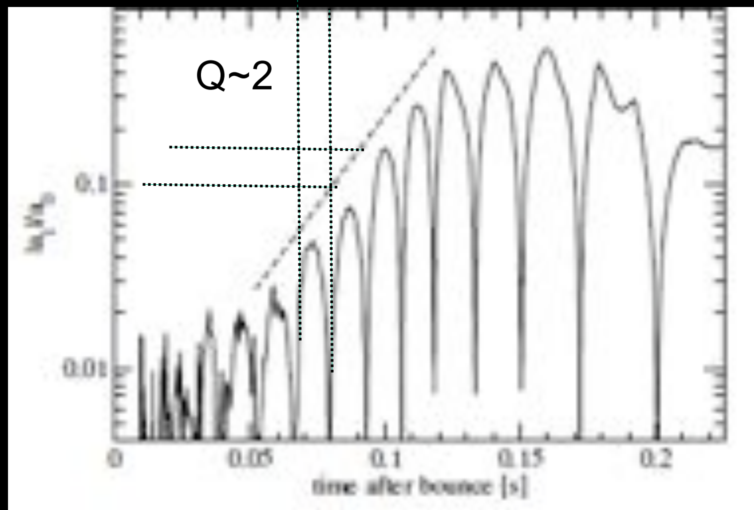

$27M_{sol}$ in 2D

Asymmetric explosion of a $15M_{sol}$ star aided by SASI

Marek & Janka 09

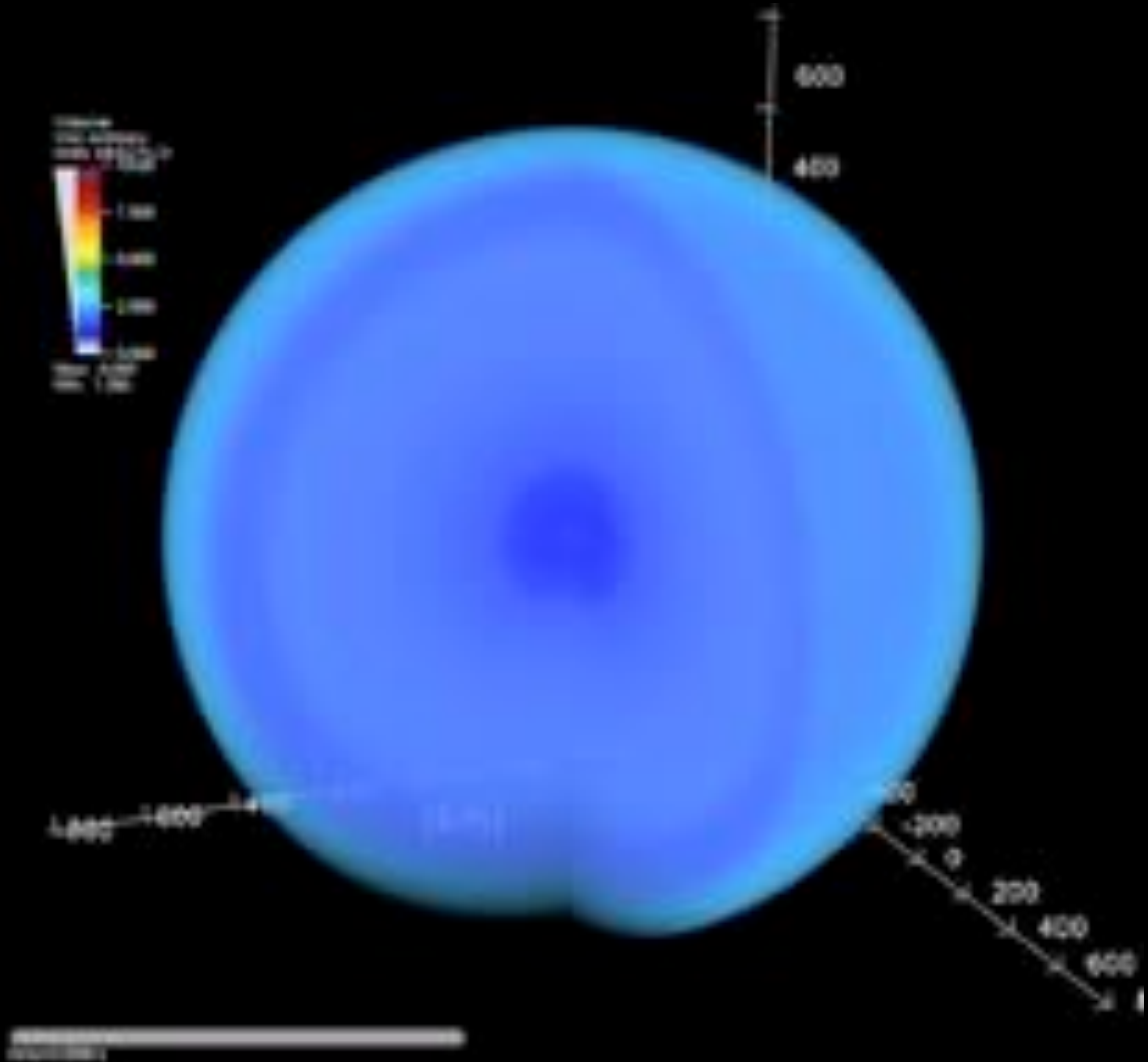

The positive effect of instabilities on the explosion threshold

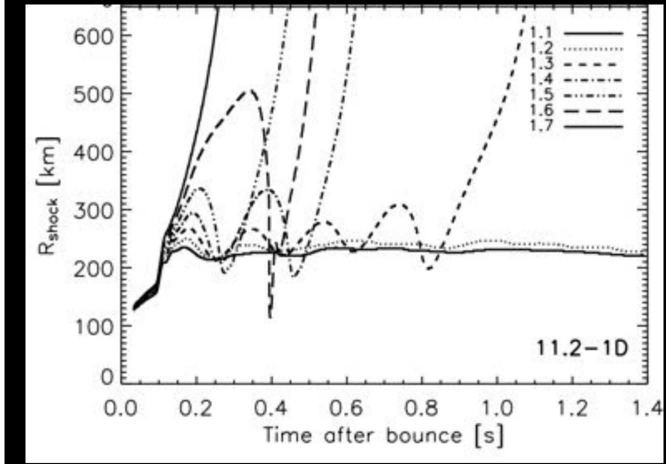

Since Burrows & Goshy 93, the explosion threshold is parametrized in the L_ν, dM/dt plane

The onset of explosion requires a high enough neutrino luminosity, or a low enough mass accretion rate.

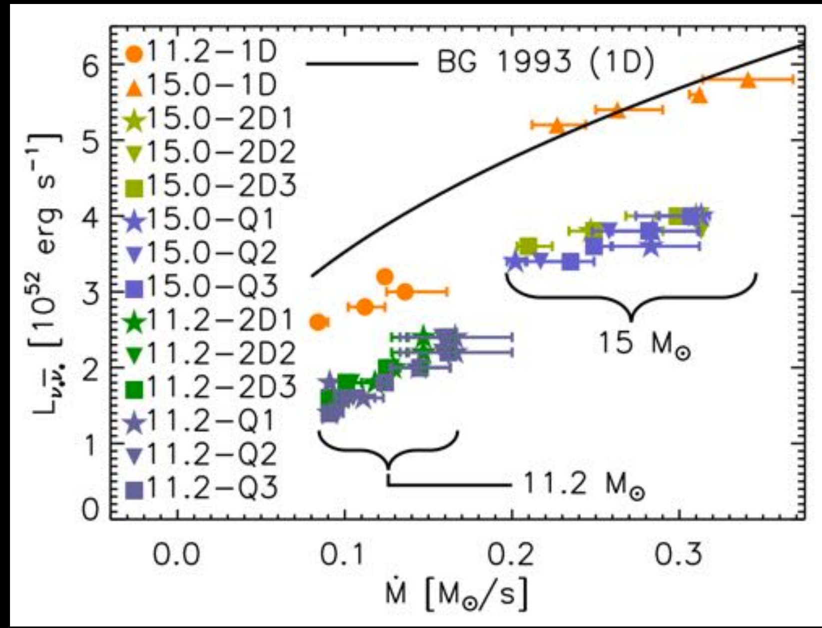

Murphy & Burrows 08

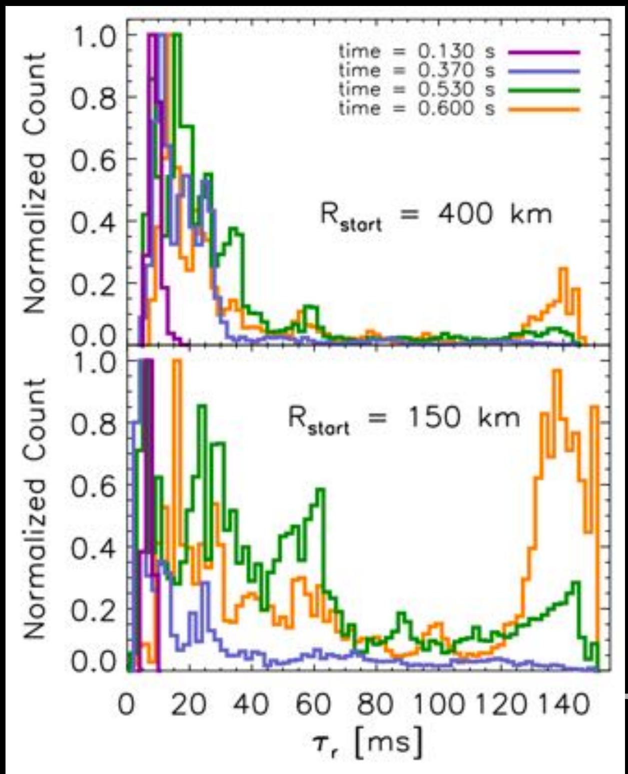

Murphy & Burrows 08 demonstrated that the SASI instability allows for explosions with a lower neutrino luminositiy threshold (-30%) than in 1D

Convective cells trap the gas and expose it to the neutrino flux for a longer time than with radial trajectories.

The contribution of turbulent pressure, either from the preshock material (Couch & Ott 15, Müller+16) or from the SASI instability (Cardal & Budiarja 16) decreases the amount of neutrino heating needed to trigger the explosion

MultiD allows for a continuous injection of accretion energy while the explosion proceeds

Significant differences in 2D ab-initio models and results

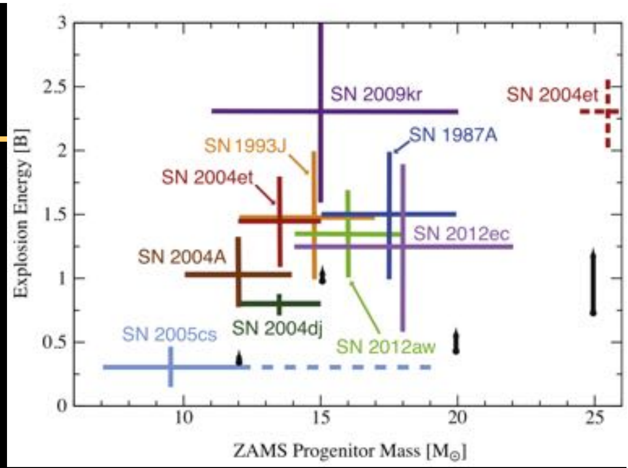

Explosions are more robust in Bruenn+16 than in Müller+13, but fail in Dolence+15

progenitor: Woosley & Weaver 95 vs Woosley & Heger 07

neutrino transport approximation: antineutrino at 200ms postbounce for $15M_{sol}$

ray by ray with MGFLD: highest antineutrino energy 19MeV (+12%), highest luminosity 55B/s (+57%) Bruenn+16

ray by ray with variable Eddington factor: intermediate energy 17MeV, lowest luminosity 35B/s

MGFLD: lowest energy 15MeV, intermediate luminosity 45B/s

IDSA (Takiwaki+14, Suwa+14, Nakamura+15)

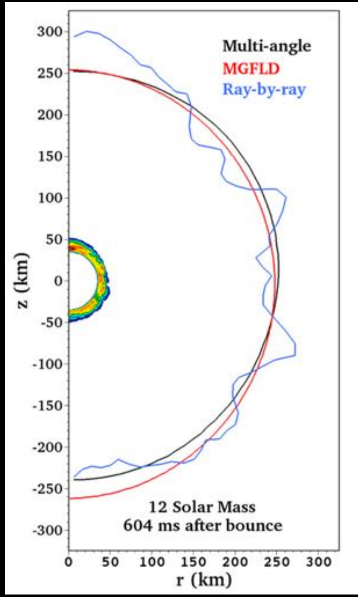

general relativity: neglected by Dolence+15

spherical GR correction in Bruenn+16, Marek & Janka 09

neutrino inelastic scattering: neglected by Dolence+15

numerical mesh: cylindrical grid seeds convection in Dolence+15

AMR may not be favourable to SASI in Dolence+15

EOS: Shen 98 in Dolence+15 is less favourable to explosions than Lattimer & Swesty 91 (Suwa+13) Dolence+15

LS180 vs LS220 + Cooperstein 85 in the postshock region

Pulsar kicks in 2D

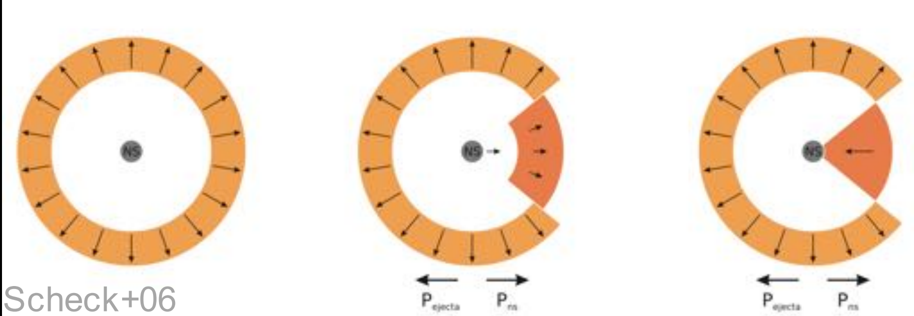

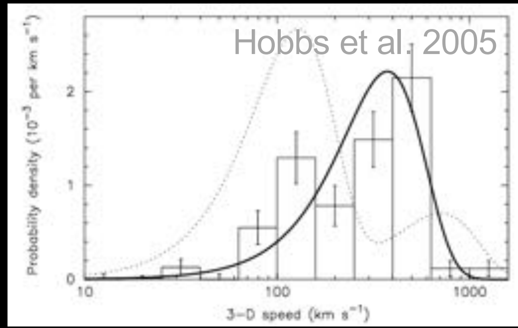

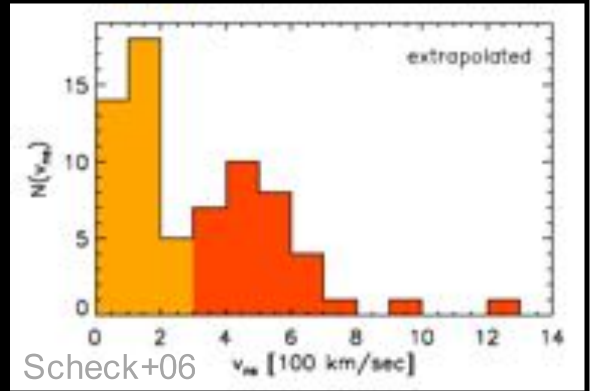

-The acceleration is mediated by the gravitational force over a longer timescale ~3s than the accretion timescale

-The kick velocity is a stochastic variable with a large dispersion

Janka+04

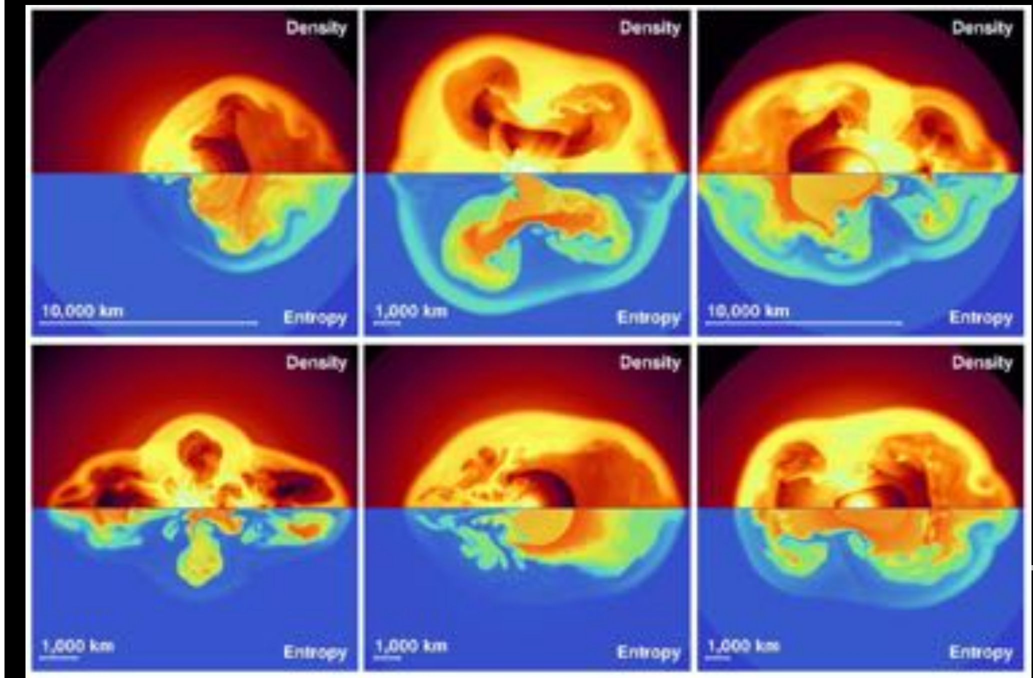

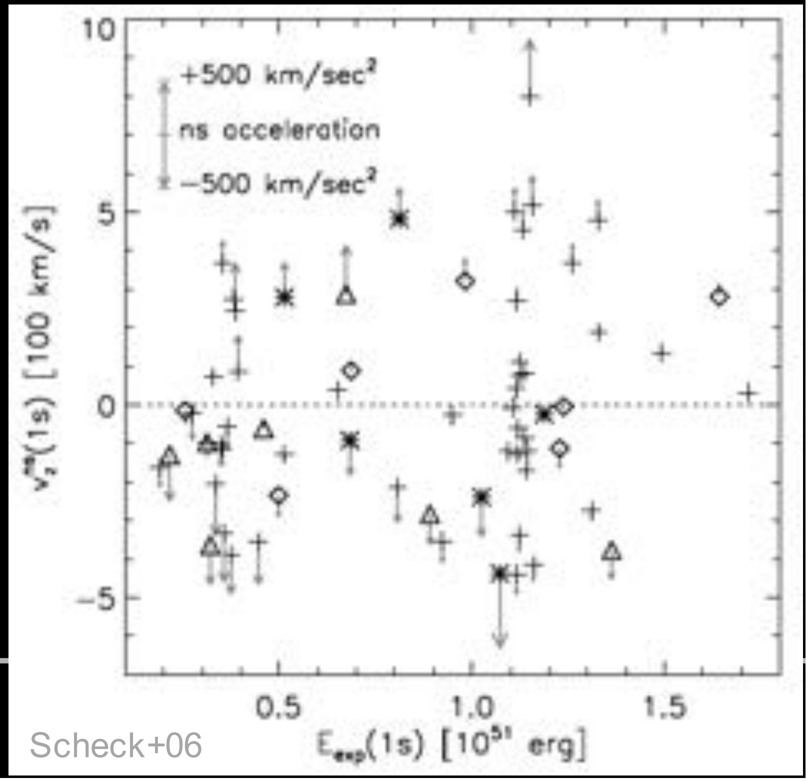

Pulsar kicks in 3D: a contradiction to kick spin alignment ?

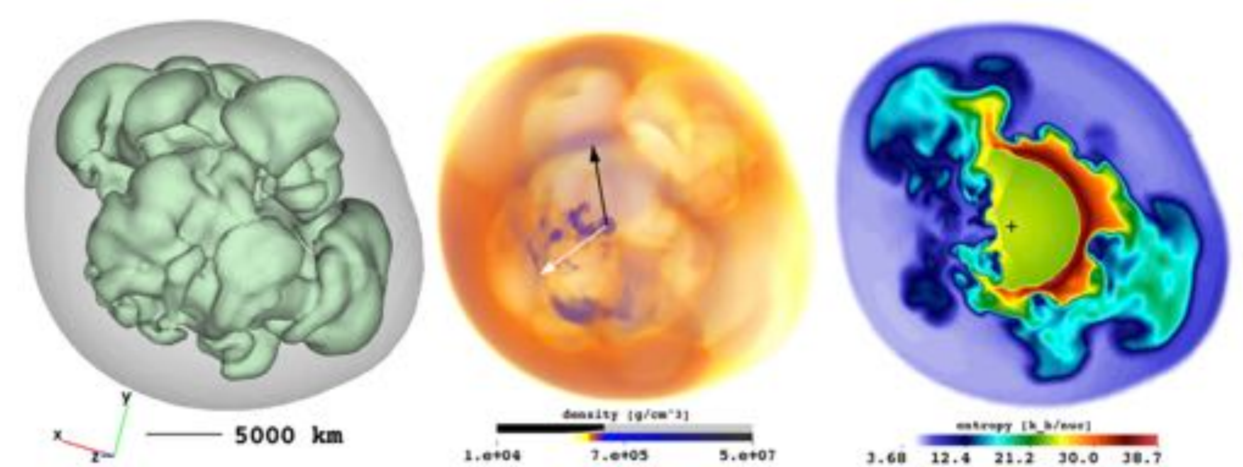

Wongwathanarat+13

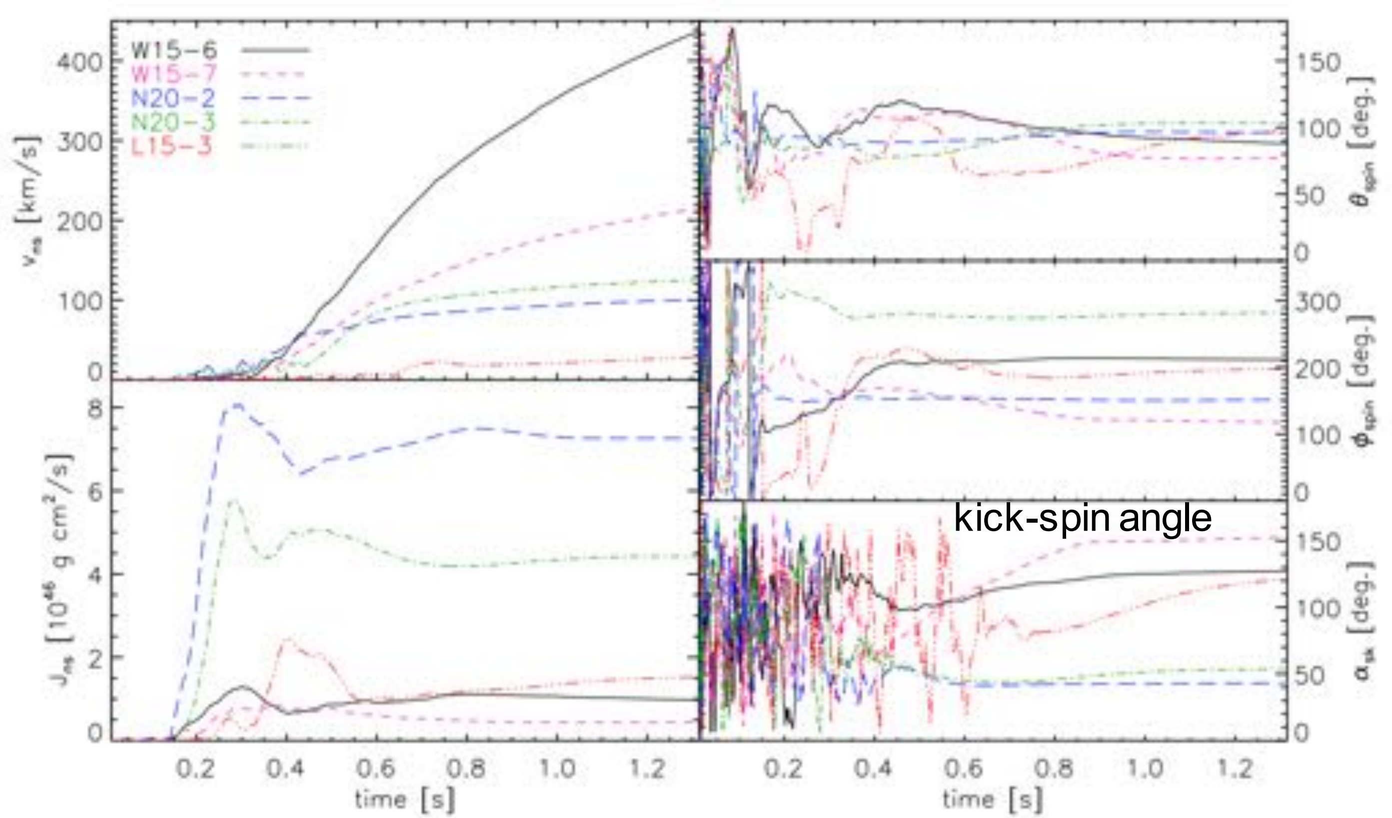

For non rotating progenitors, the kick-spin angle seems uniformly distributed.

The spin is gained from the accretion of the asymmetric flow (t<0.6s).

The kick is gained on a longer timescale (t~1-3s) from the gravitational interaction with the aspherical ejecta.

3D simulations of rotating progenitors are needed to conclude about the kick-spin correlation

Gravitational waves signatures from non axisymmetric features

(Ott+06, Kotake+07, Marek+09, Ott 08, Murphy+09, Kotake+11, 13, E.Müller+12, B.Müller+13, Hayama+15, Kuroda+14, +16)

Low T/W spiral modes of fast spinning cores produce strong gravitational waves (e.g. Hayama+15)

Model	Ω_{ini} (rad s^{-1})	$\rho_{max,b}$ (10^{14} g cm^{-3})	β_b
R0	0	3.54	2.3×10^{-5}
R1	$\pi/6$	3.52	1.5×10^{-3}
R2	$\pi/2$	3.41	1.3×10^{-2}
R3	π	3.28	4.9×10^{-2}

For a non rotating progenitor, the stochastic wobbling of the SASI spiral mode axis weakens the GW signature in 3D compared to 2D.

Nevertheless, the SASi induced GW signal is sensitive to the compactness of the core, the equation of state (Müller+13, Kuroda+16), and the rotation rate (Kotake+11, Kuroda+14).

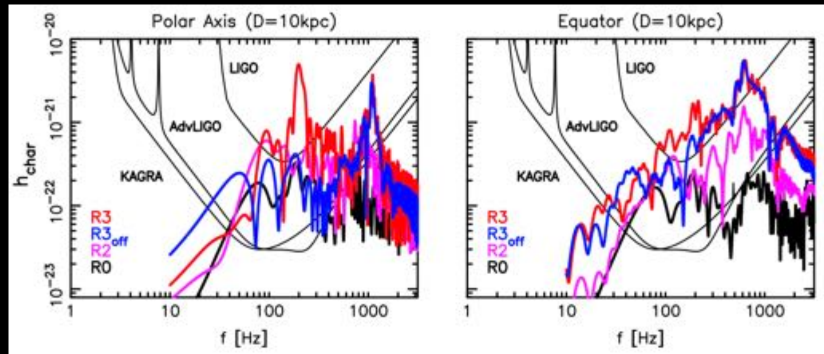

Kuroda+16

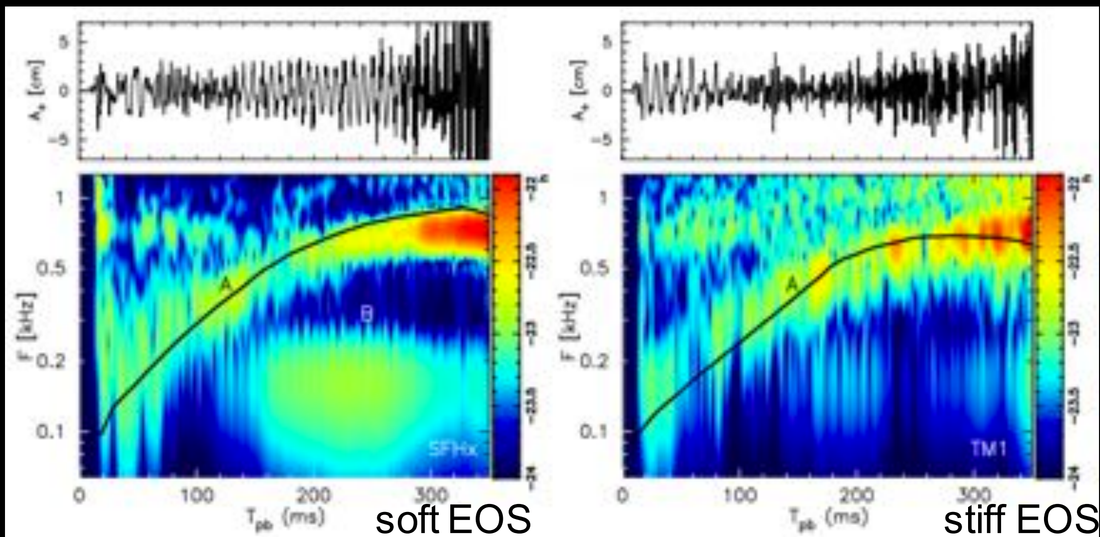

detection by LIGO, KAGRA for a non rotating galactic supernova at 10kpc:

g-mode activity with S/N=10
SASI activity with S/N~50

A: NS g-mode oscillations (600-700Hz)
B: SASI activity (100-200Hz)

Neutrino signature of 3D instabilities

(Marek+09, Müller+12, Lund+10, +12, Tamborra+13, +14, Müller & Janka 14)

$$\bar{\nu}_e + p \rightarrow n + e^+$$

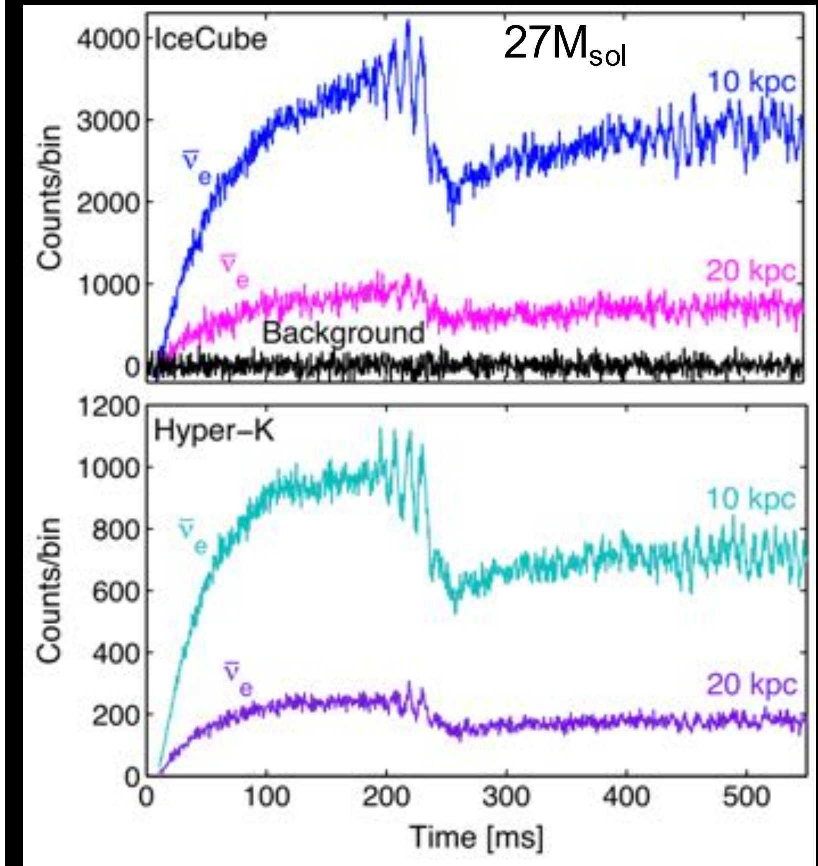

Tamborra+13

For a galactic supernova at 10kpc:

IceCube will detect 10^6 events above the background
Super-K (32kton): 10^4 events
Hyper-K (740kton): 3×10^5 events background free

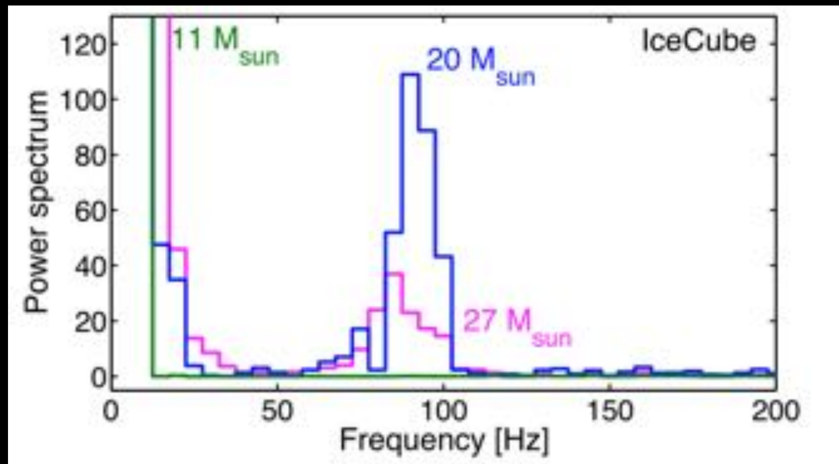

→direct signature of the SASI oscillation frequency

The end of a controversy: the existence of SASI in 3D

-despite Burrows+12a,b, Murphy+13, Dolence+13,
SASI can be dominant even in the most realistic 3D simulations: $27M_{sol}$ progenitor
(Hanke+13)

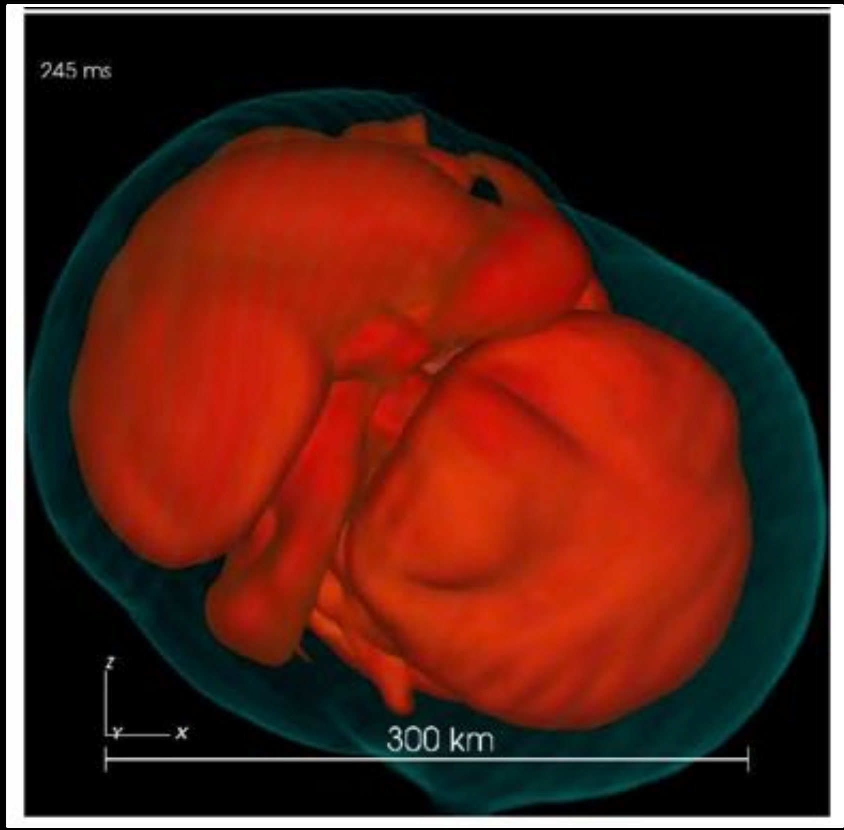

$27M_{sol}$ on the verge of explosion in 3D

-The first 3D ab initio simulation of $27M_{sol}$ did not explode after 380ms (Hanke+13)

... but a minor change in the nucleon strangeness was enough to produce an explosion (Melson+15)

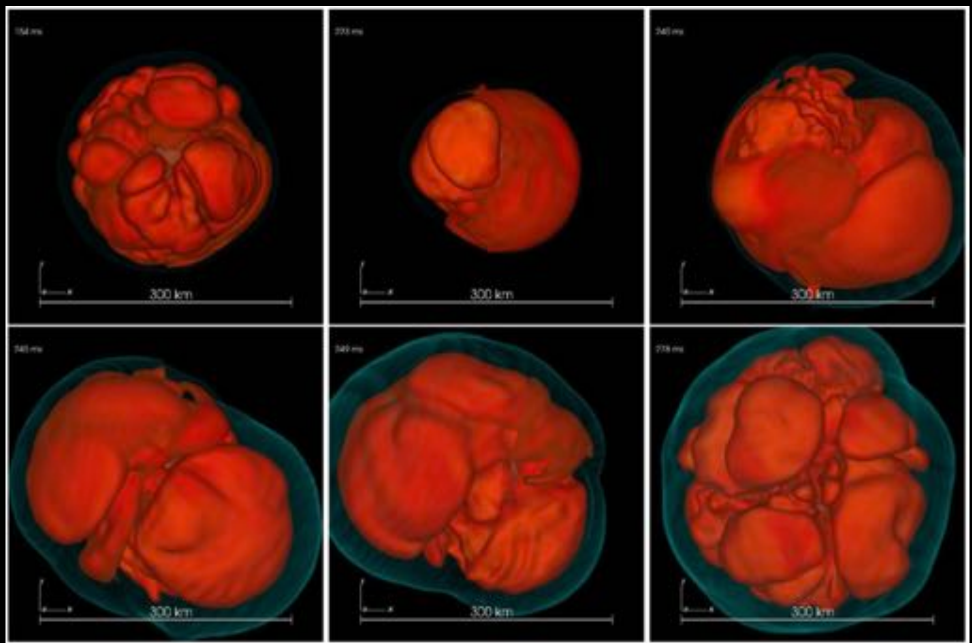

Hanke+13

project PRACE 150 millions hours
16.000 processors, 4,5 months/model

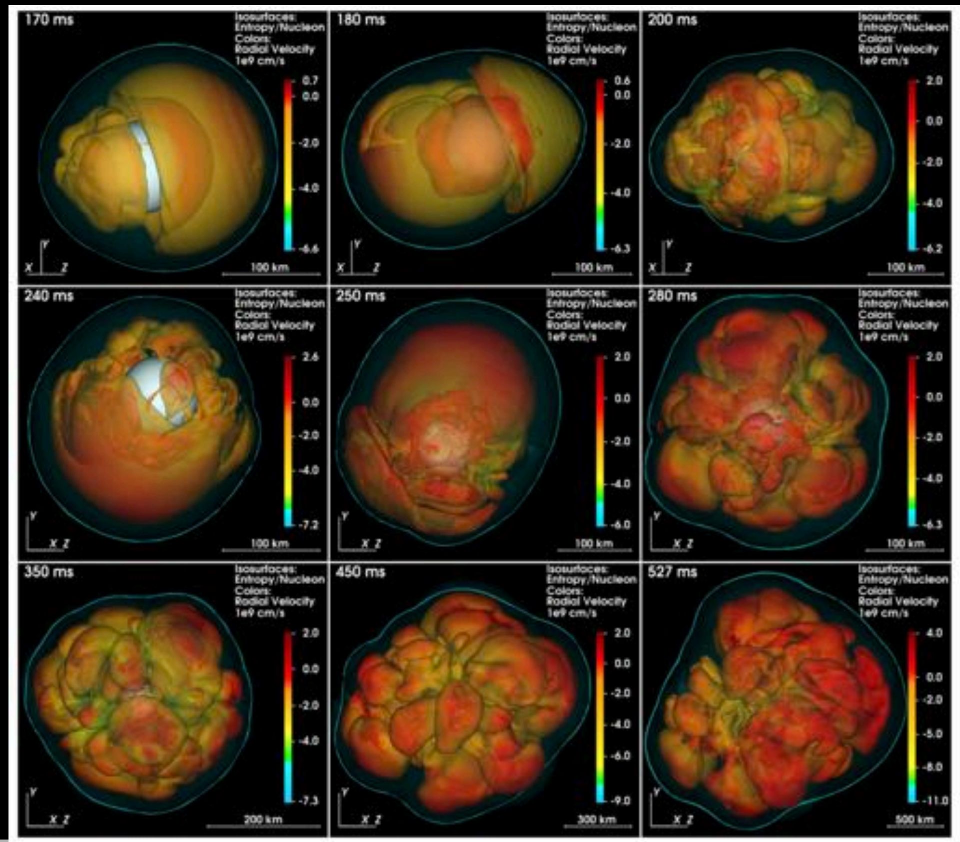

Melson+15

Growing evidence that 3D explosions are more difficult than in 2D?

-Contrary to Nordhaus+10, Dolence+13, explosion is not obviously easier in 3D than in 2D (Hanke+12, Couch & O'Connor 13)

-Inverse turbulent cascade in 2D favours the build up of larger scale motions than in 3D

-27M_{sol} did not explode in 3D (Hanke+13) but exploded in 2D (Müller+12)
-11.2M_{sol} exploded less energetically in 3D than in 2D (Takiwaki+14)
-15M_{sol} exploded later in 3D than in 2D (Lentz+15)

Lentz+15

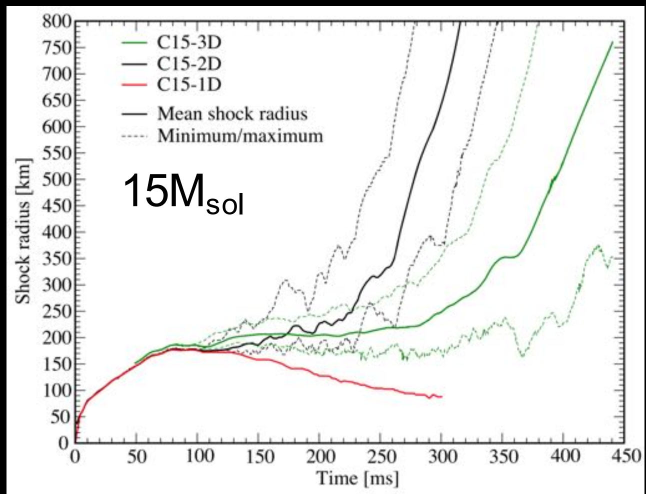

Takiwaki+14

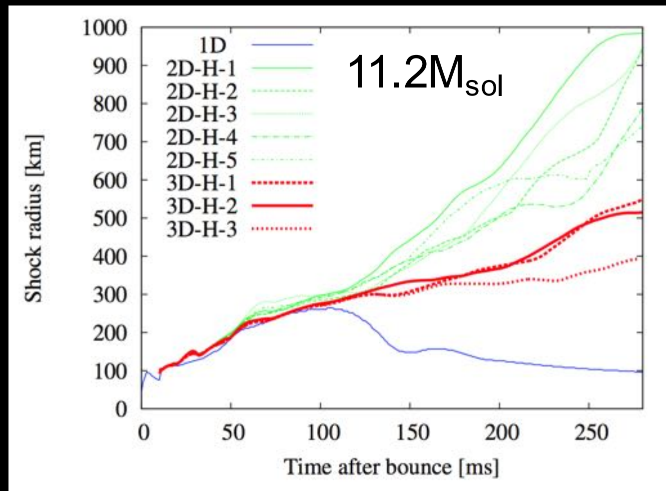

but...

-convection in 3D may better resist advection than in 2D (Kazeroni+17)

-3D SASI (27M_{sol}, Hanke+13) should be strengthened even by modest rotation (Yamasaki & Foglizzo 08)

Outline of lecture 5

Impact on the explosion & new ideas

Two paths to explosion & signatures

2D-3D debate

Rotation effects: from SASI to low T/W

Magnetic effects: magnetic SASI, MRI

How much angular momentum in a stellar core?

From the observation of pulsars in supernova remnants, the estimated distribution of spin period at birth is flat from 10ms to 100ms (Popov & Turolla 12), Without any redistribution of angular momentum the specific angular momentum of the stellar core would be

$$j_{\rm NS} \equiv R^2\Omega = 2.1\times10^{14}\left(\frac{R}{10{\rm km}}\right)^2\left(\frac{P}{30{\rm ms}}\right)^{-1}{\rm cm^2\ s^{-1}}$$
$$= 6.3\times10^{15}\left(\frac{R}{10{\rm km}}\right)^2\left(\frac{P}{1{\rm ms}}\right)^{-1}{\rm cm^2\ s^{-1}}$$

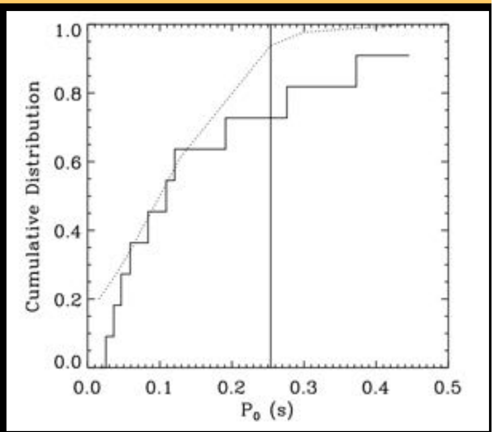

Popov & Turolla 12

From stellar evolution including magnetic prescription for the transport of angular momentum the typical spin period of a pulsar should be P~15ms ($j\sim4\times10^{14}cm^2s^{-1}$) within a factor 2 uncertainty (Heger+05)

Asterosismic observations of low mass red giants suggest that stellar interiors rotate slower than predicted by theoretical models: theoretical prescriptions for transport processes seem to underestimate the efficiency of transport (Cantiello+14)

Internal gravity waves may be able to regulate the angular momentum of the core and produce pulsars with slower periods (Fuller+15)

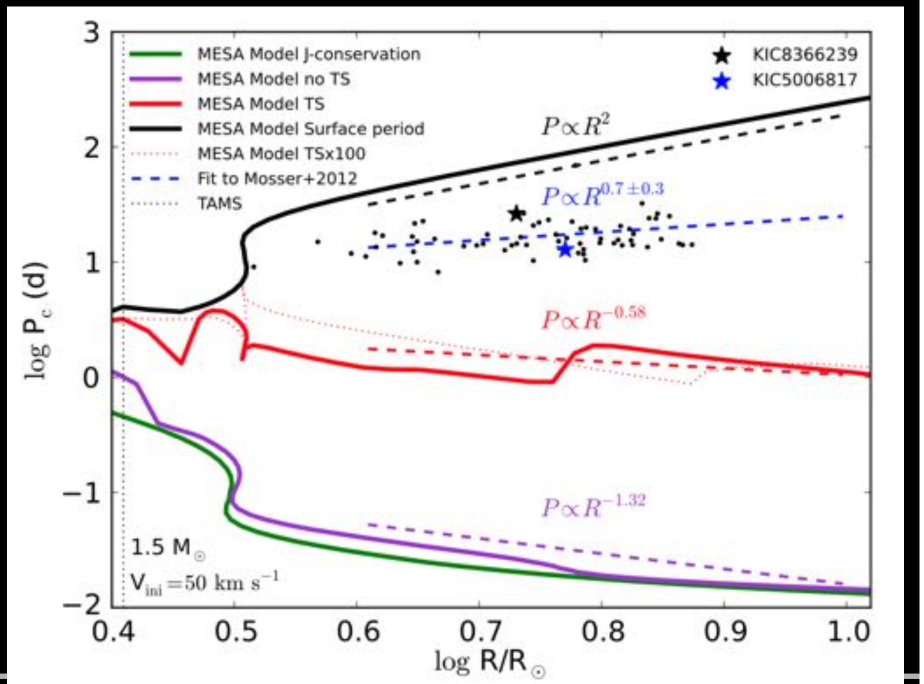

Cantiello+14

Very few simulations include rotation

SASI

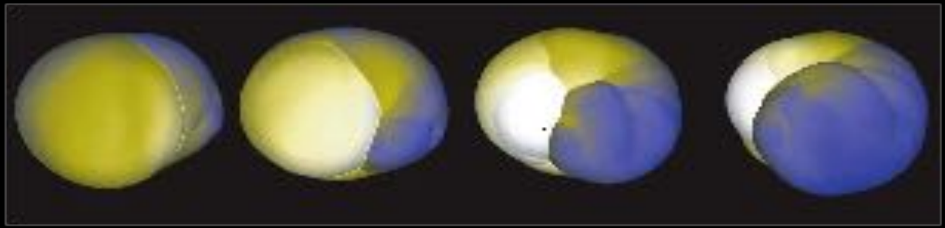

(Blondin & Mezzacappa 07)

$j = 10^{15}$ cm^2/s or $P_0 = 6$ ms

"Slow" rotating progenitor

Low-T/|W|

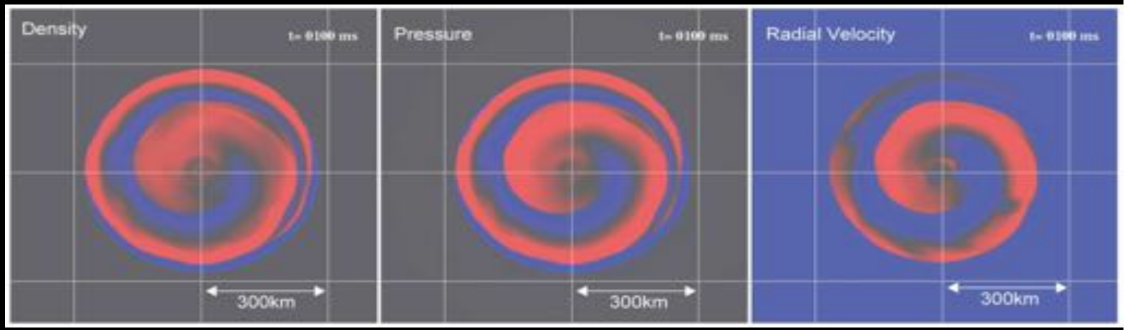

(Takiwaki+16)

$j = 4.10^{16}$ cm^2/s or $P_0 \approx 0.15$ ms

"Fast" rotating progenitor

stellar evolution favours: $j \sim 10^{15}$ cm^2/s (e.g. Heger+05)

What about intermediate rotation rates ?

Rotating progenitor: redistribution of angular momentum by SASI

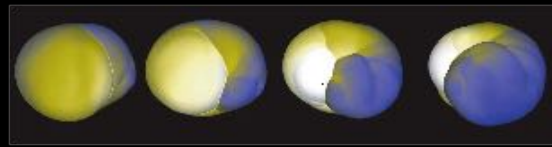

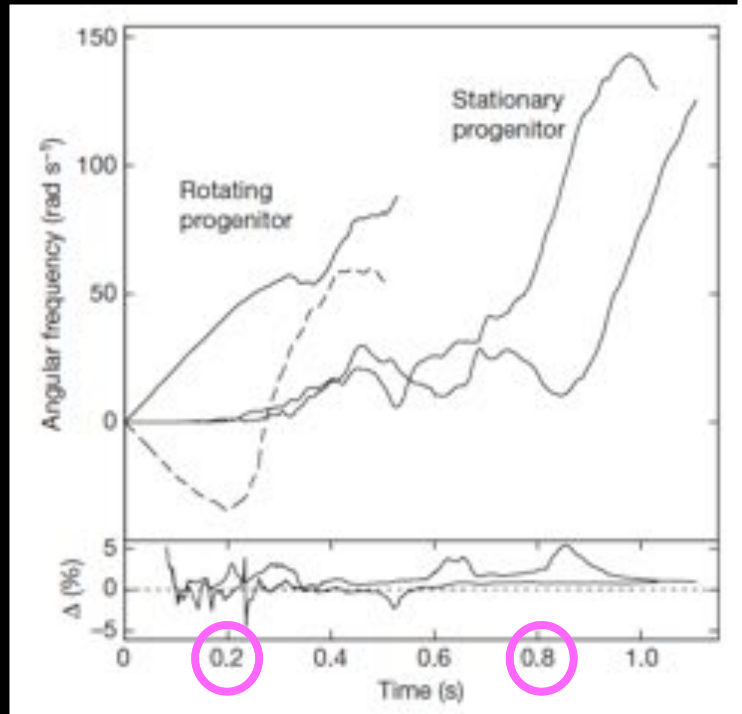

Blondin & Mezzacappa 07

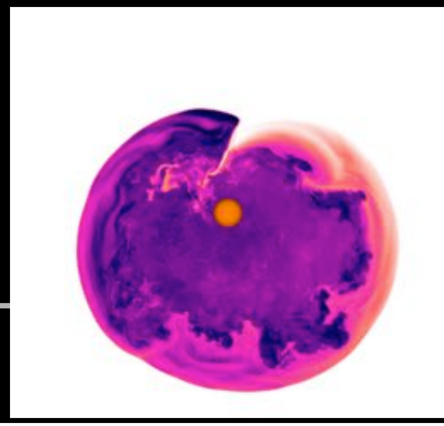

rotation period: 246s
injection slit: 0.55mm
flow rate: 1.17L/s

Effect of core rotation on SASI in a cylindrical flow

(Yamasaki & Foglizzo 08)

- Growth rate of the spiral mode

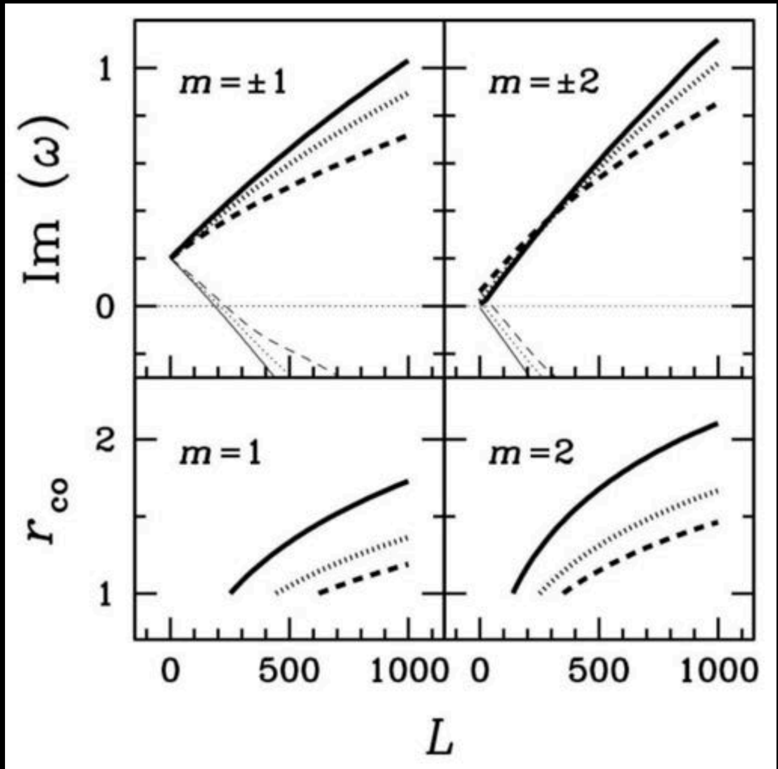

Even if the centrifugal force is dynamically negligible, differential rotation influences directly the prograde spiral mode of SASI through the Doppler shifted frequency ω-mΩ

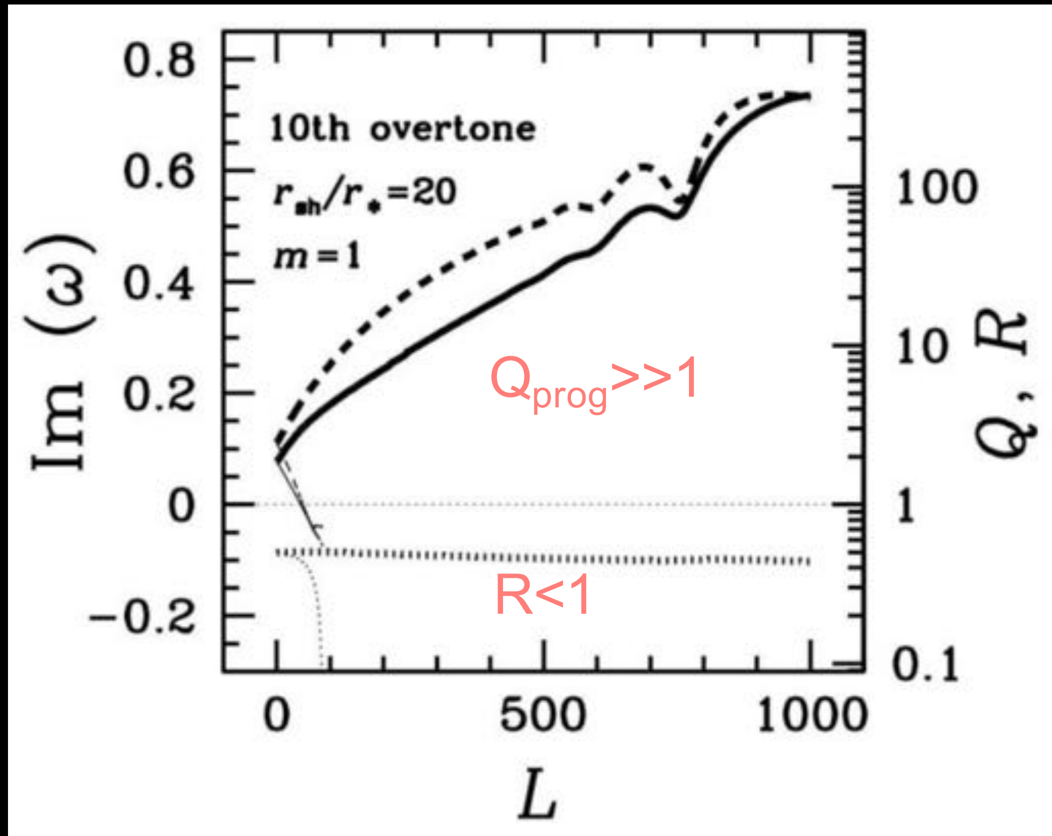

WKB analysis: the acoustic mode is stable.

Why is the prograde advective-acoustic mode so much favoured?

Comparison of rotation effects on shallow water equations and gas dynamics

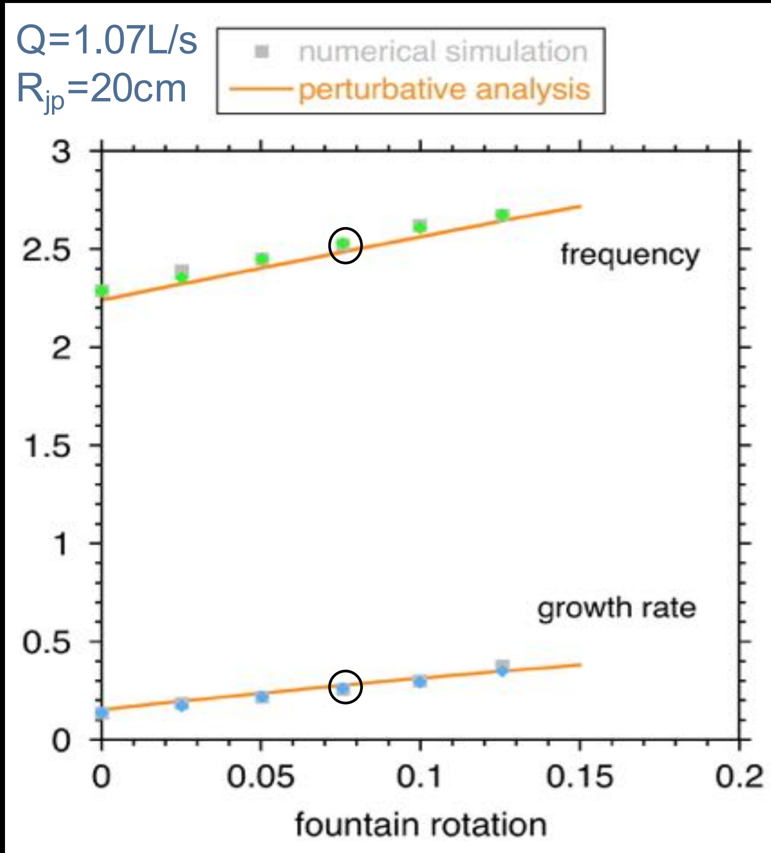

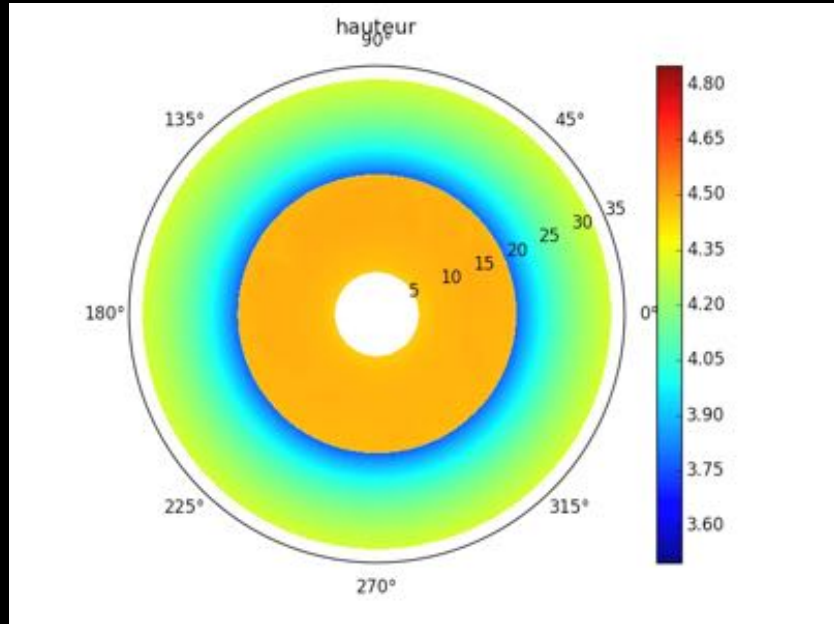

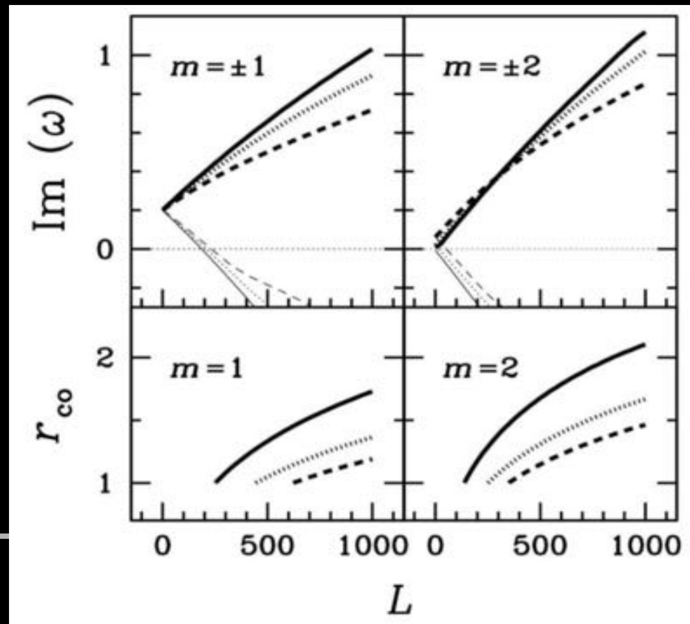

Yamazaki & Foglizzo 08

same linear increase of the growth rate as in YF08, despite
- the absence of buoyancy effects
- γ=2 instead of γ=4/3
- accreting inner boundary

What is the physical mechanism of this rotational destabilization?

Experimental growth rates are measured using the contrast of the hydraulic jump

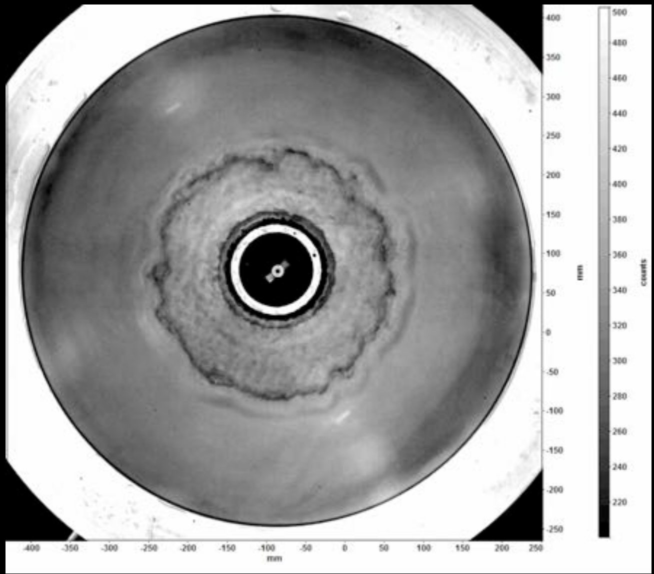

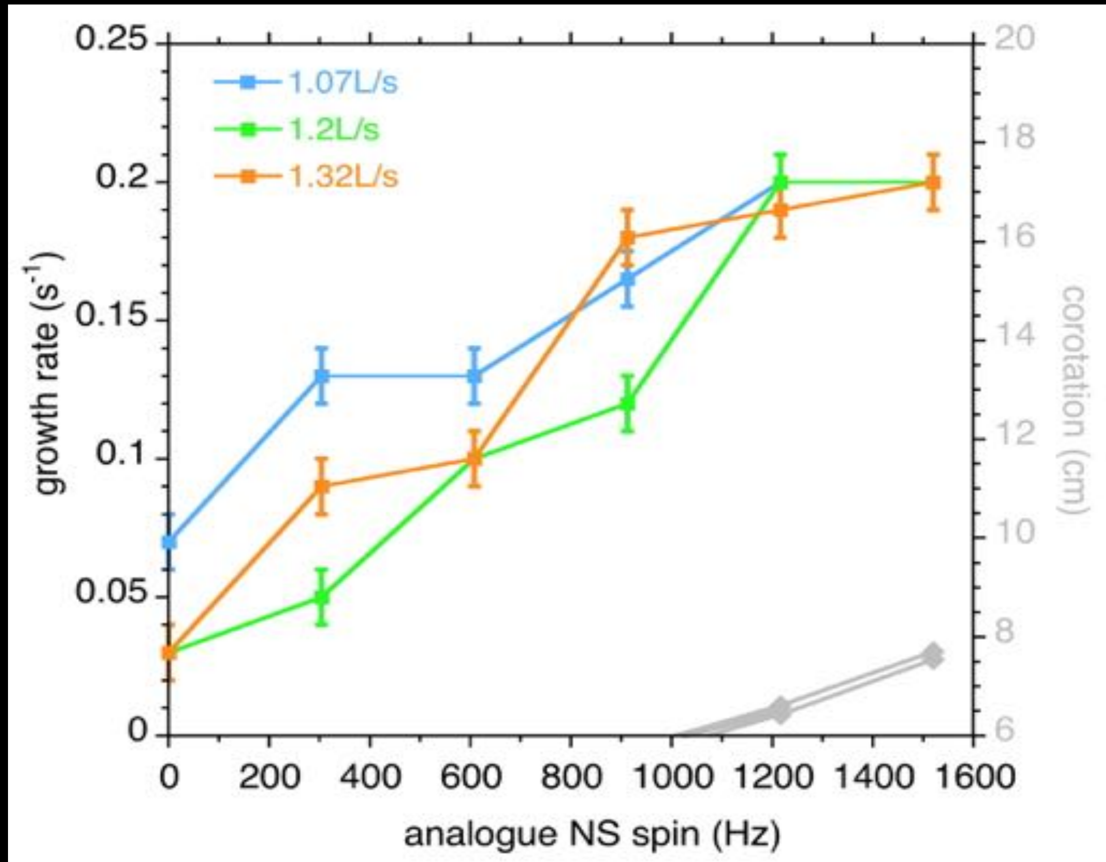

- increase of the growth rate with rotation
- m=2 dominates m=1 for fast rotation

Comparison of the experiment with the shallow water equations

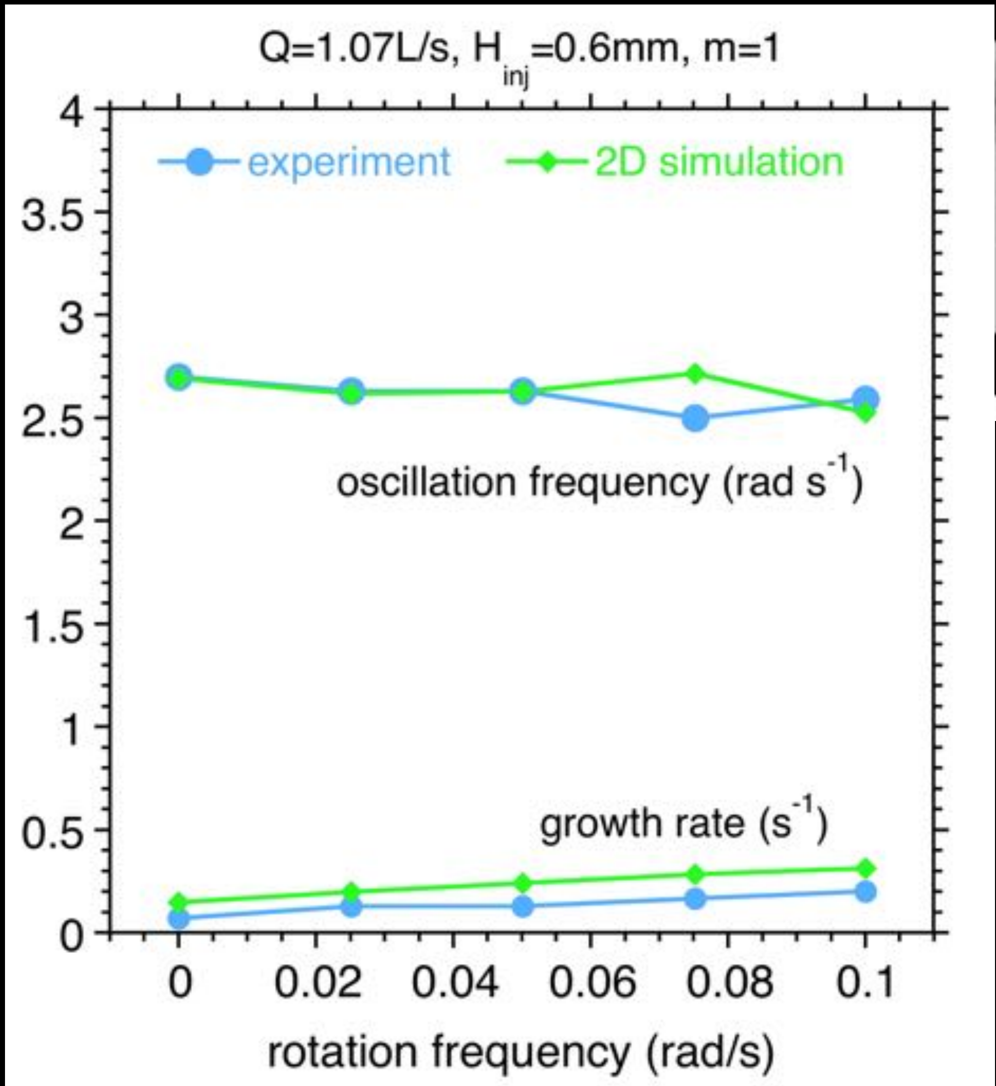

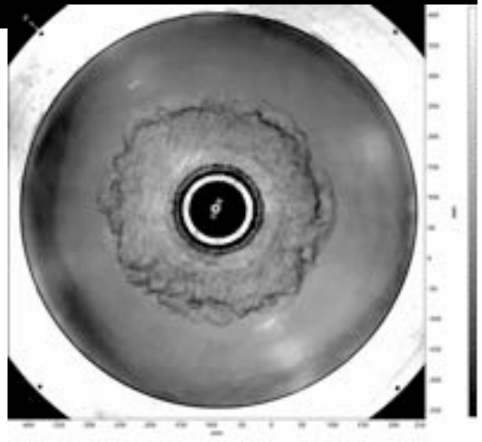

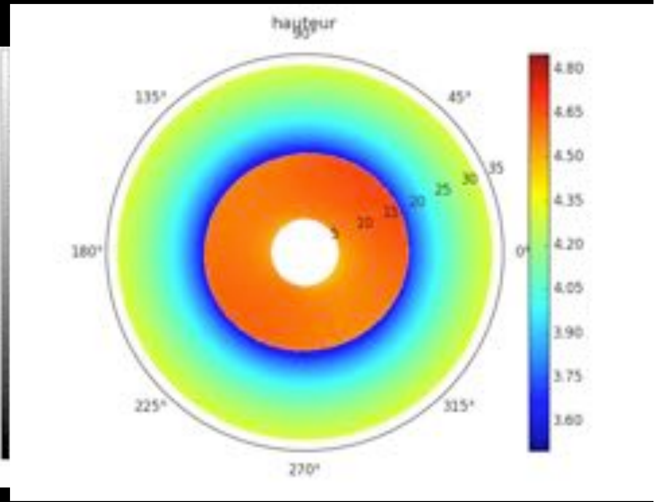

-surprisingly good agreement, despite
- -2D shallow water modeling,
- -laminar drag without any free parameter,
- -ignoring turbulence,
- -ignoring surface tension,
- -ignoring the radial extension of the jump

-experimental growth rates are systematically lower by $\Delta\omega_i \sim 0.2\ s^{-1}$

Beyond the shallow water approximation: phase mixing of dragged vorticity ?

$$\mathrm{Re}_H \equiv \frac{Hv}{\nu} = 796 \left(\frac{Q}{1\mathrm{L/s}}\right)\left(\frac{20\mathrm{cm}}{R_{\mathrm{jump}}}\right) = 2650 \left(\frac{Q}{1\mathrm{L/s}}\right)\left(\frac{6\mathrm{cm}}{R_{\mathrm{NS}}}\right)$$

$$\mathrm{Re}_L \equiv (R_{\mathrm{inj}} - R_{\mathrm{jump}})\frac{v_{\mathrm{inj}}}{\nu} = 10^5 \left(\frac{Q}{1\mathrm{L/s}}\right)\left(\frac{0.6\mathrm{mm}}{H_{\mathrm{inj}}}\right)$$

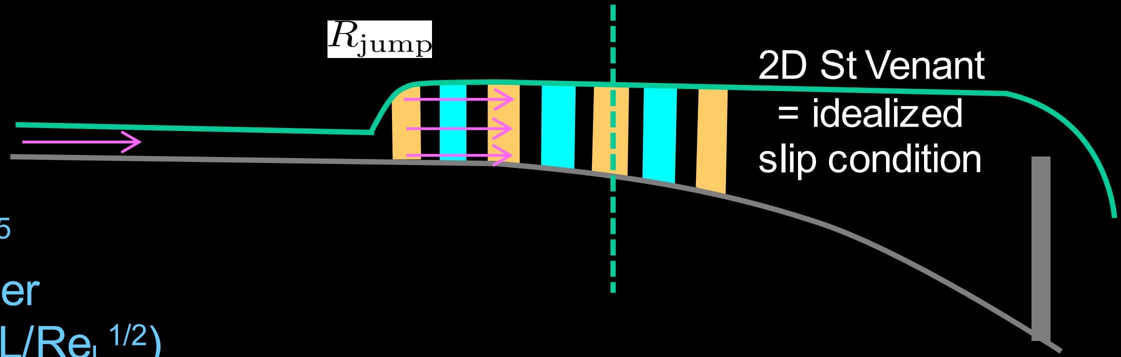

ill-defined vertical structure H(R)

-laminar/turbulent transition $\mathrm{Re}_L \sim 5\times10^5$

-vertical extension of the boundary layer

$\delta_{jp} \sim 2$mm if laminar ($4.91\ L/\mathrm{Re}_L^{1/2}$)

$\delta_{jp} \sim 5$mm if turbulent ($0.38\ L/\mathrm{Re}_L^{1/5}$)

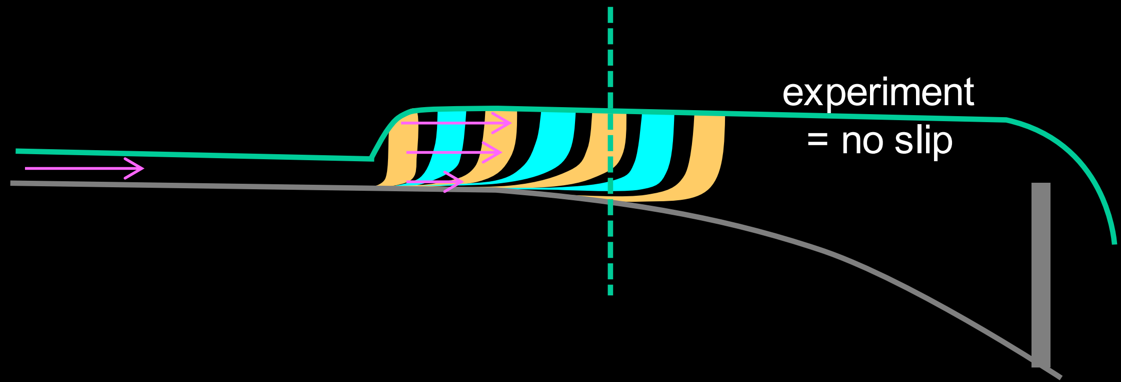

reference examples

-half-Poiseuille: $\frac{v(z)}{<v>} \sim \frac{3z}{2H}\left(2 - \frac{z}{H}\right)$

-turbulent prescription: $\frac{v(z)}{<v>} \sim \frac{8}{7}\left(\frac{z}{H}\right)^{\frac{1}{7}}$

The vertically averaged vorticity is damped by a factor Q

$$Q \sim \int_0^H \frac{\mathrm{d}z}{H} \cos\left[\frac{\omega_{\mathrm{SASI}}\Delta R}{v(z)}\right] \sim 0.27 \text{ (laminar)}$$
$$\sim 0.52 \text{ (turbulent)}$$

Increasing the rotation rate (20% Kepler) : a robust spiral shock driven at the corotation radius

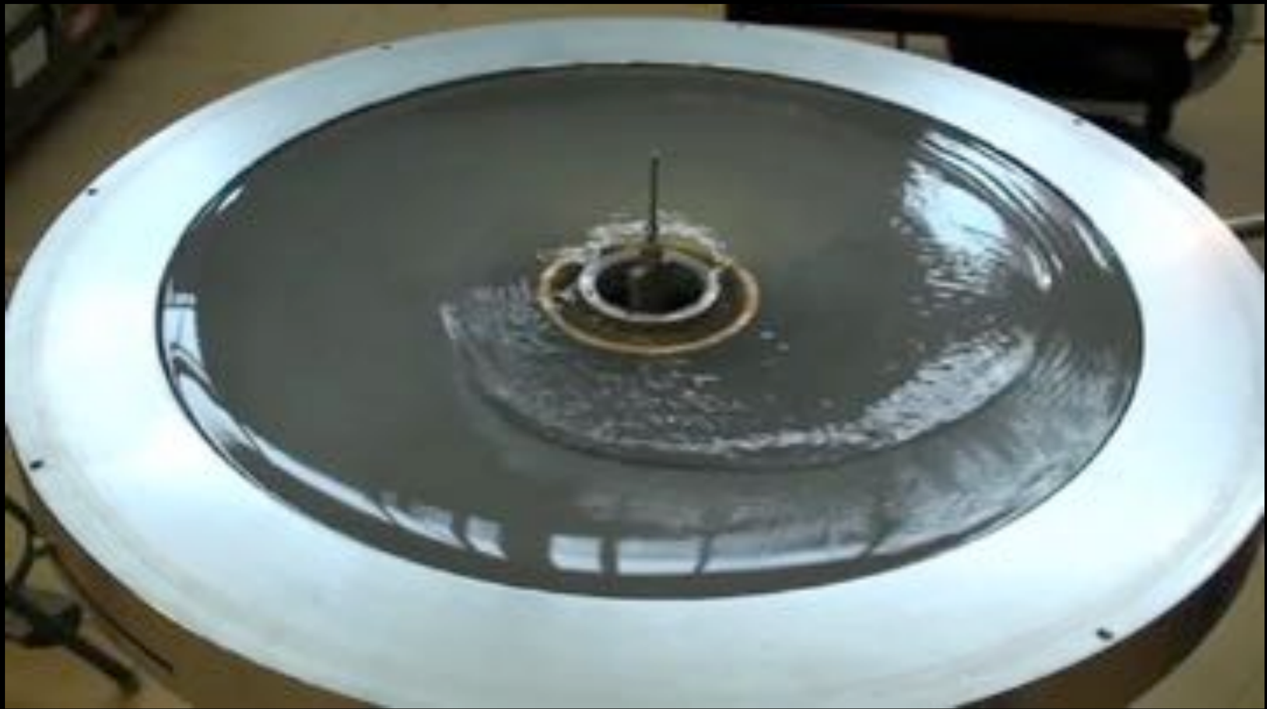

flow rate: 0.3L/s, slit size: 1.6mm

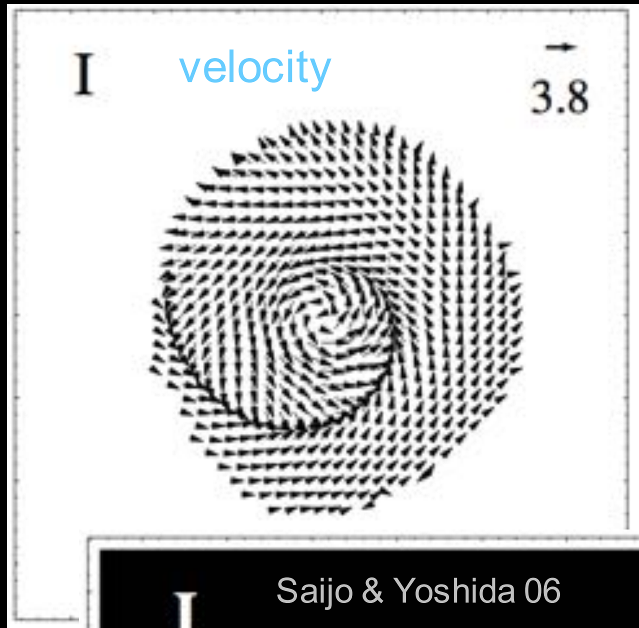

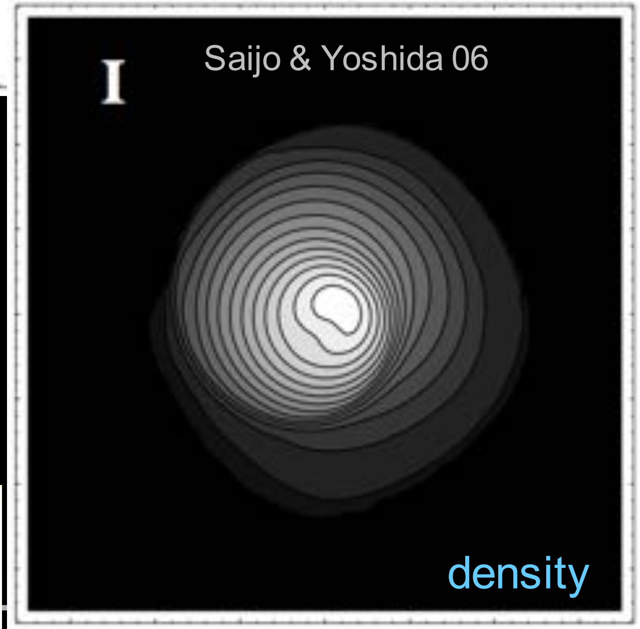

analogue to the “low T/W” instability of a neutron star rotating differentially
(Shibata+02,03, Saijo+03,06, Watts+05, Passamonti & Andersson 15)

boundary conditions are different in stellar core-collapse:
- inner advection
- outer accretion shock

recent 3D simulations by Takiwaki+16

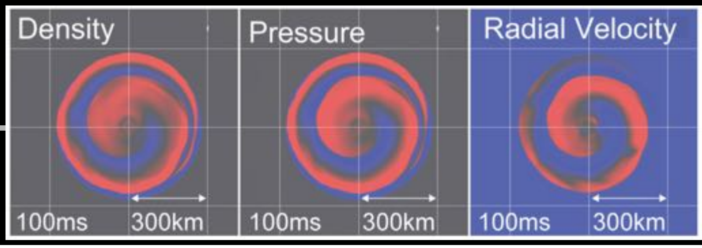

The corotation instability

Goldreich & Narayan 85

The dispersion relation of acoustic waves in a uniform gas with a uniform velocity v_0 along x

$(\omega - k_x v_0)^2 = k^2 c_0^2$ is rewritten in a rotating fluid with differential rotation $\Omega(r)$ using a local reference frame in cylindrical coordinates (r,θ)

A model equation is the parabolic cylinder equation (Goldreich & Narayan 85)

$$\frac{d^2 v}{dX^2} + \left(\frac{1}{4}X^2 - C\right) v = 0$$

The wavenumber of the acoustic perturbation is approximated as $(k_r, m/r)$

$$(\omega - m\Omega)^2 \sim \left(k_r^2 + \frac{m^2}{r^2}\right) c^2 \quad \rightarrow \quad k_r^2 \sim \frac{1}{c^2}(\omega - m\Omega)^2 - \frac{m^2}{r^2}$$

The fluid at the corotation radius r_{corot} rotates with the same phase velocity as the wave pattern $\Omega(r_{corot})=\omega/m$

Acoustic waves are evanescent in the corotation region, delimited by two turning points r_t^+, r_t^- defined by $k_r=0$

$$\Omega(r_t) \sim \Omega_c \pm \frac{c}{r_t}$$

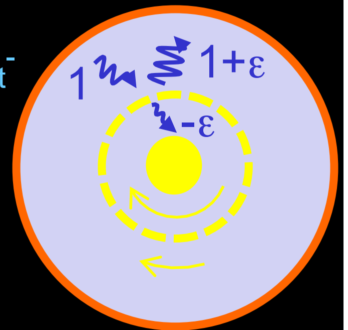

The azimuthal velocity of the fluid is -faster than the wave pattern at $r<r_{corot}$

-slower than the wave pattern at $r>r_{corot}$

An acoustic wave carrying some azimuthal momentum in the direction of rotation increases the kinetic energy of the fluid for $r>r_{corot}$ and decreases it for $r<r_{corot}$

Evanescent propagation across the corotation region decreases the negative energy of the outer wave while increasing the positive energy of the inner wave: the outer wave is over-reflected as it approaches the outer turning point.

The corotation instability requires a reflecting boundary to close the amplification loop.

The corotation instability in core-collapse accretion

The description of over-reflected acoustic waves is limited to high frequencies to satisfy the WKB approximation

In a differentially rotating neutron star, the low T/W instability has been identified as a corotation instability of the fundamental acoustic mode l=m=2 (Passamonti & Andersson 15)

The corotation instability is expected to exist in a flow with radial accretion and a shock but the theory is missing and its interplay with SASI is not understood yet (Kuroda+14): transition from an advective-acoustic cycle to a purely acoustic cycle ?

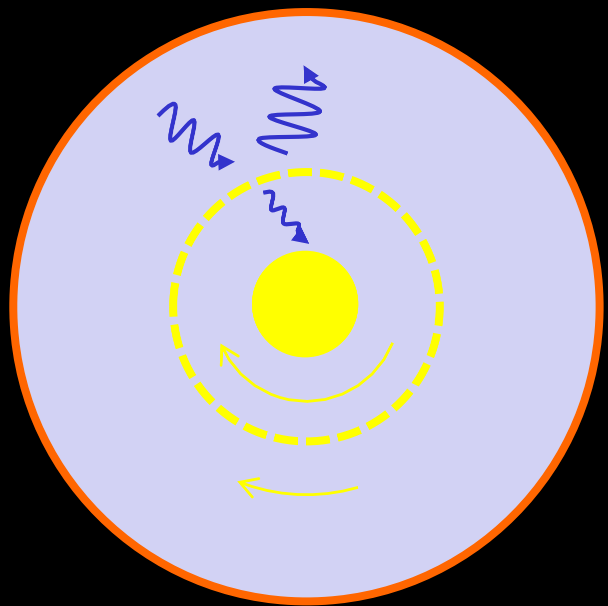

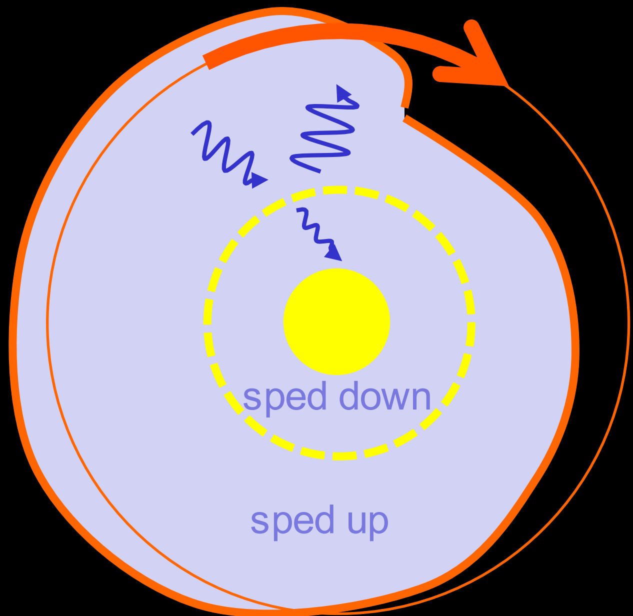

Evidence for a corotation radius using a PIV analysis

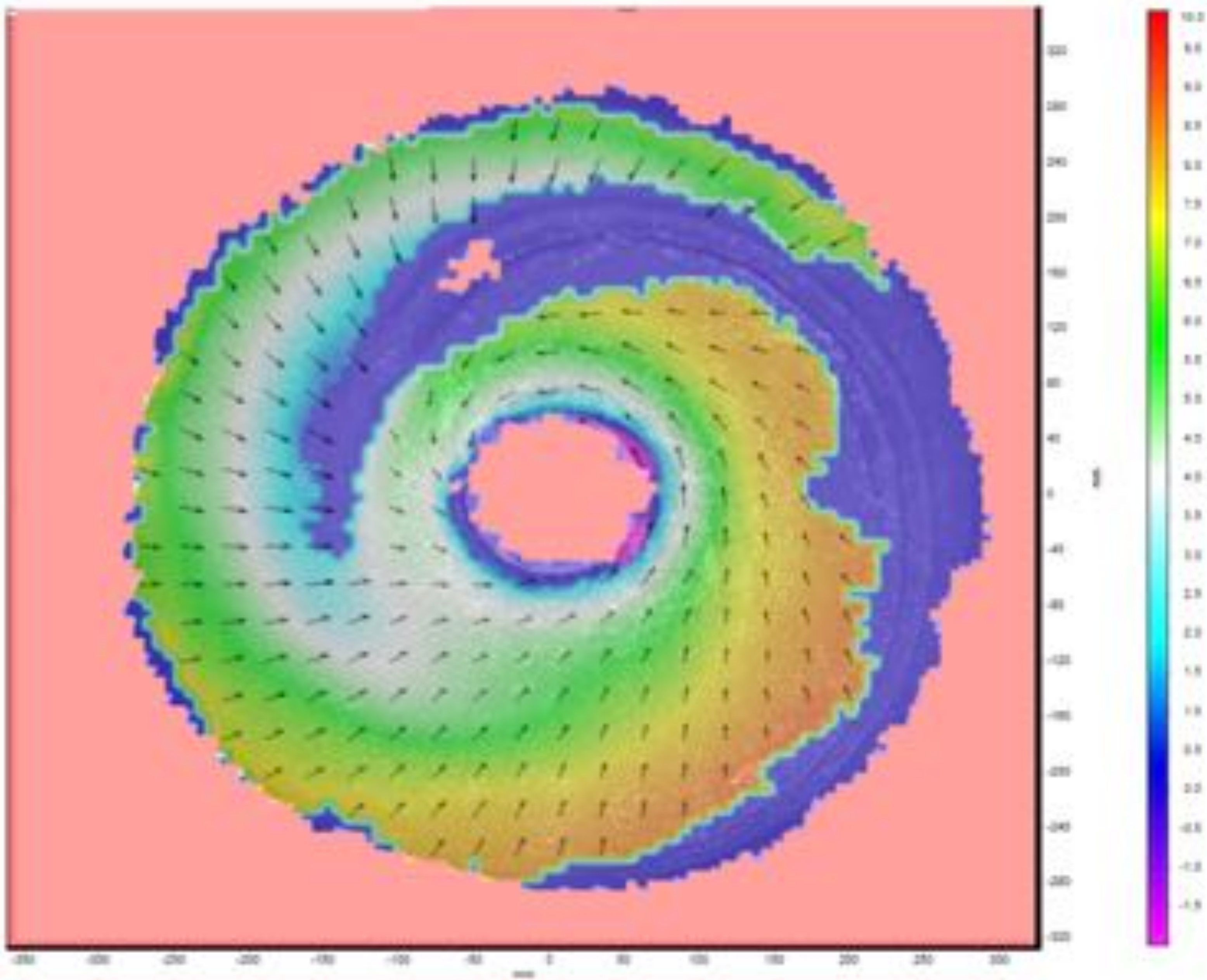

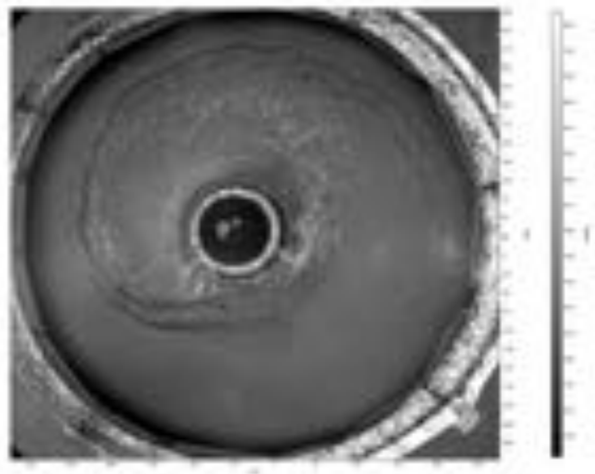

stereo measurement
of the free surface
height and velocity

Evidence for a corotation radius using a PIV analysis

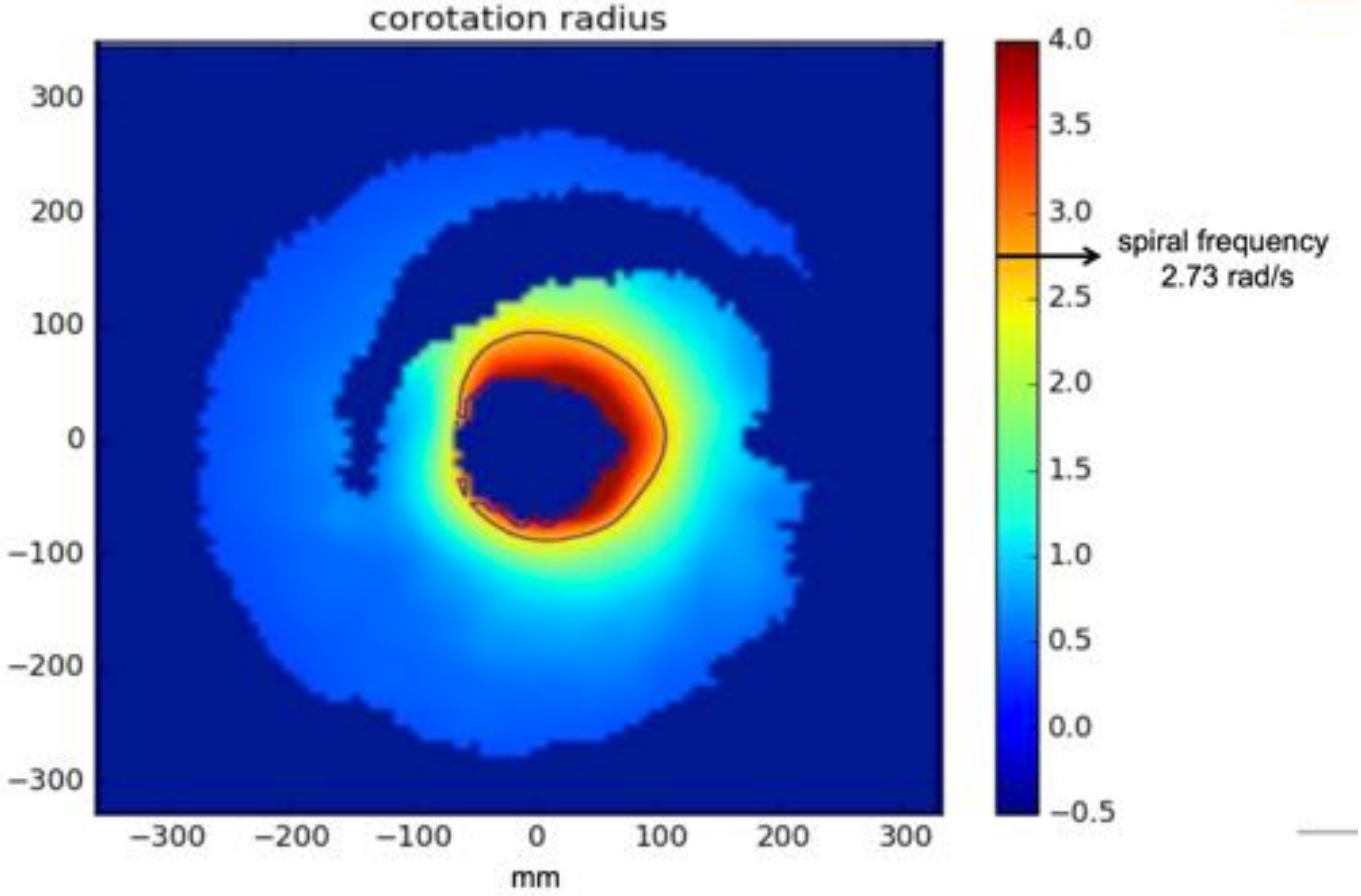

Gradual increase of the rotation rate:
continuous transition from SASI to the corotation instability

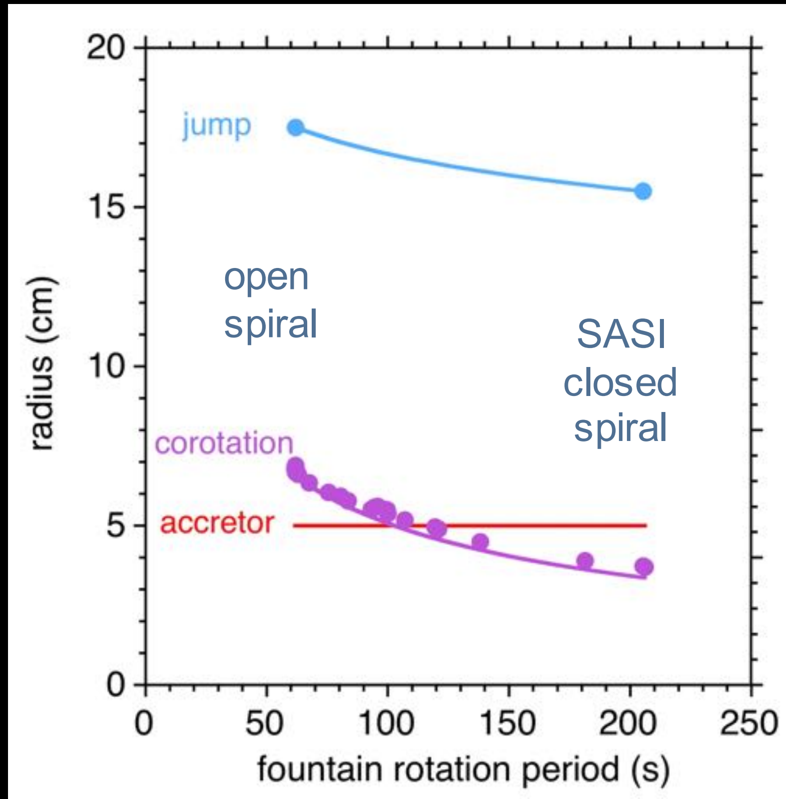

injection slit: 0.55mm
fountain rotation period: gradually decreased from 205s to 62s
flow rate: gradually decreased from 1.1 L/s to 0.59 L/s

Corotation radius and the low T/W instability

Kazeroni+17

$R_{sh}/R_{NS} = 5$

$j = 10^{15}$ cm²/s

SASI

$j = 6.10^{15}$ cm²/s

Low-T/|W|

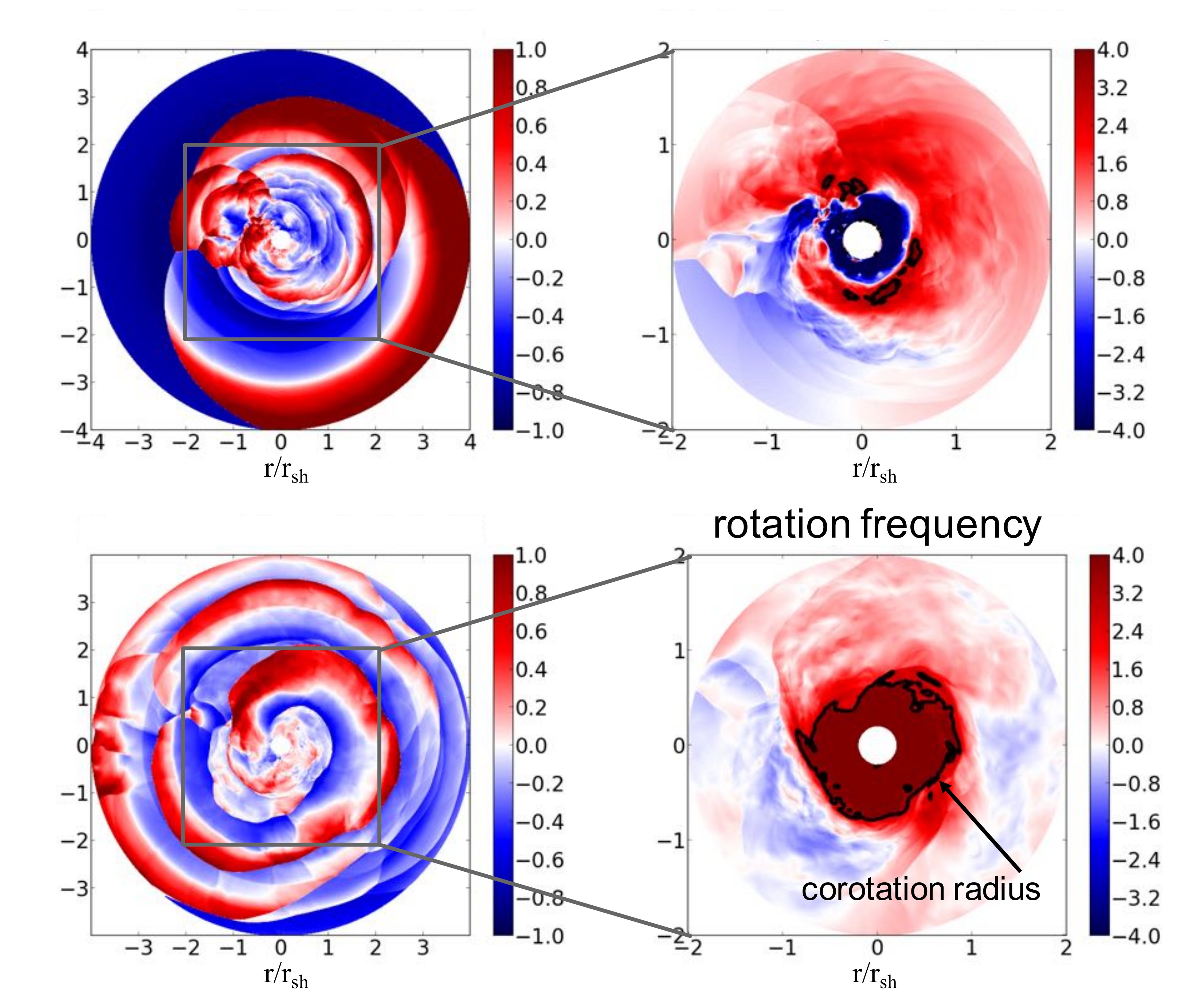

Spin-up or spin-down of the neutron star?

(Kazeroni+17)

2D cylindrical simulations of shocked accretion with a cooling function

SASI alone

Neutron Star rotation frequency

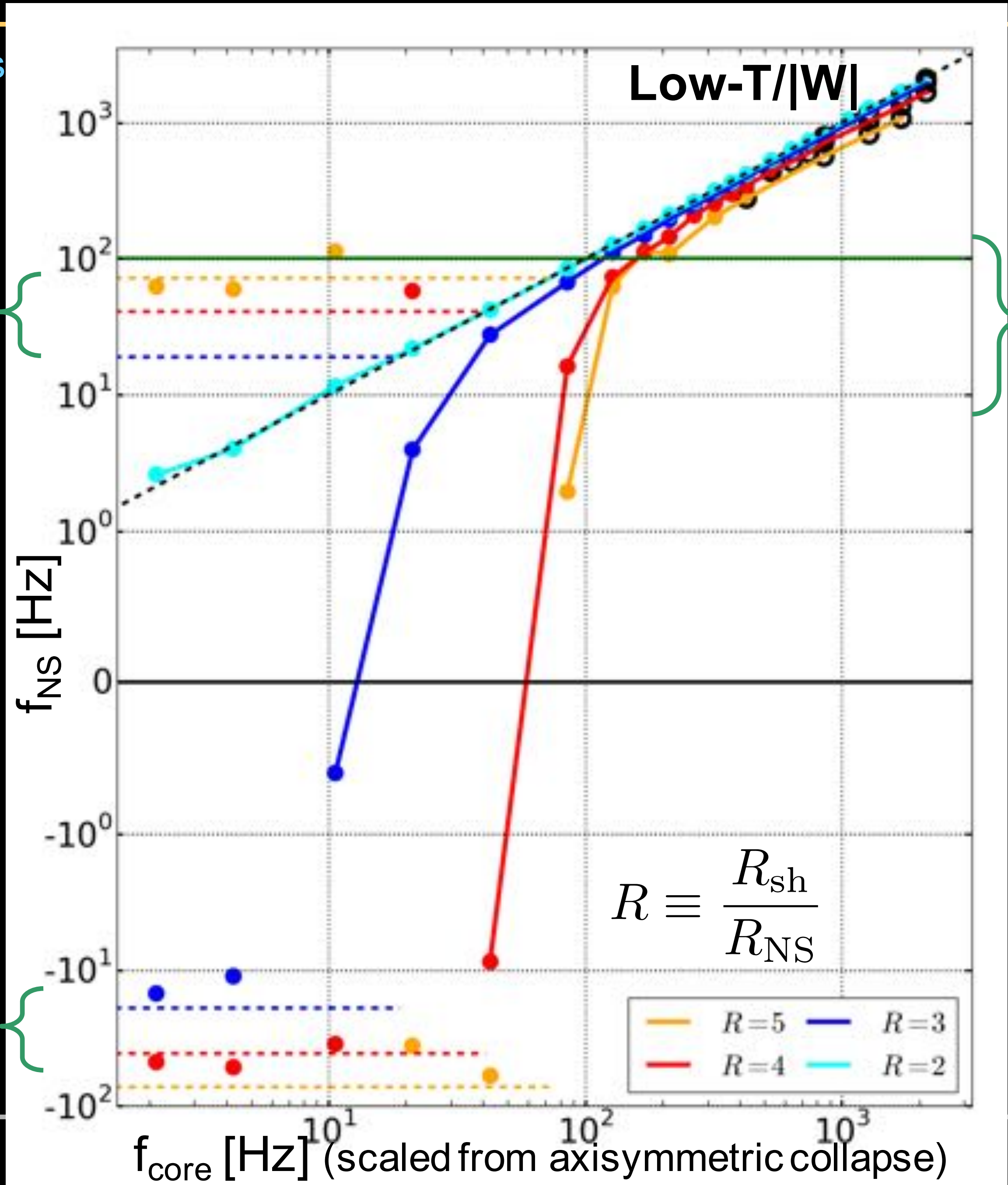

SASI alone

range of NS spin at birth

For a strong rotation rate, the corotation instability decelerates the neutron star by less than 40%.

Outline of lecture 5

Impact on the explosion & new ideas

Two paths to explosion & signatures

2D-3D debate

Rotation effects: from SASI to low T/W

Magnetic effects: magnetic SASI, MRI

Magnetic effects: wave coupling

Guilet & Foglizzo 10

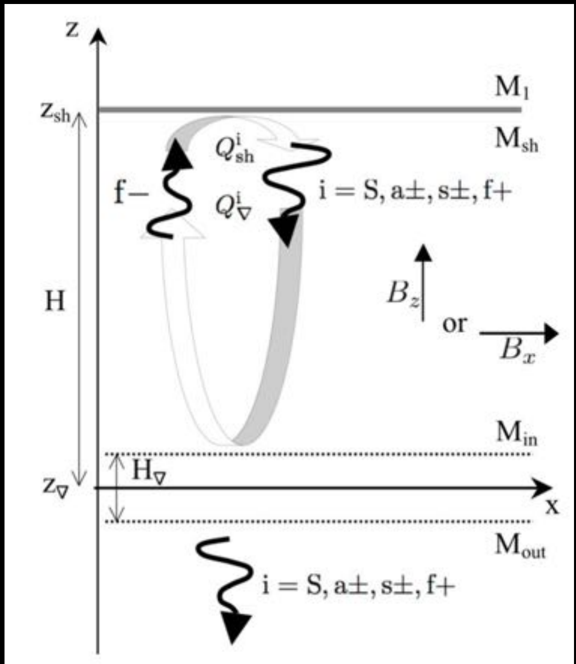

In a large scale magnetic field, the mechanism of SASI is enriched by Alfven waves, slow and fast magnetosonic waves. Entropy and vorticity perturbations are no longer advected in phase, because vorticity perturbations are propagated as Alfven waves. The main consequence is a loss of phase coherence of the advective-acoustic cycle (Guilet & Foglizzo 10).

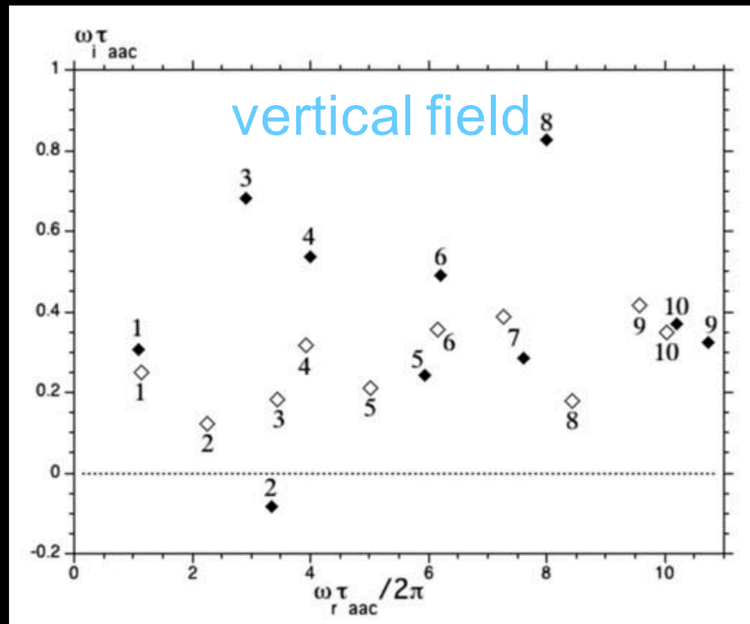

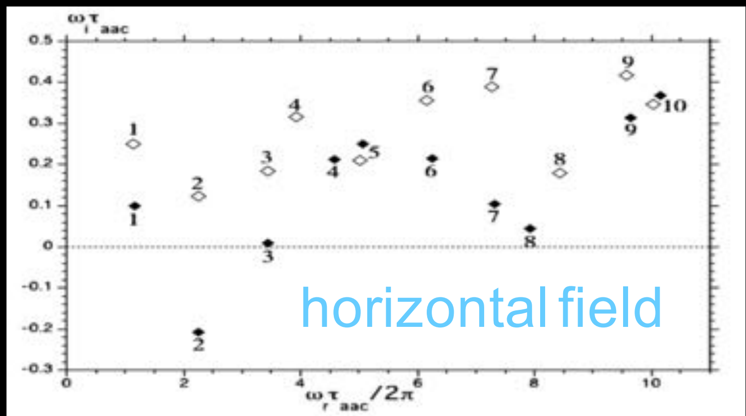

Magnetic effects: the Alfven point

Guilet+11

The Alfven point defines the point where the flow velocity equals the Alfven velocity. Upward propagating Alfven waves accumulate at this point and dissipate into heat (Guilet+11).

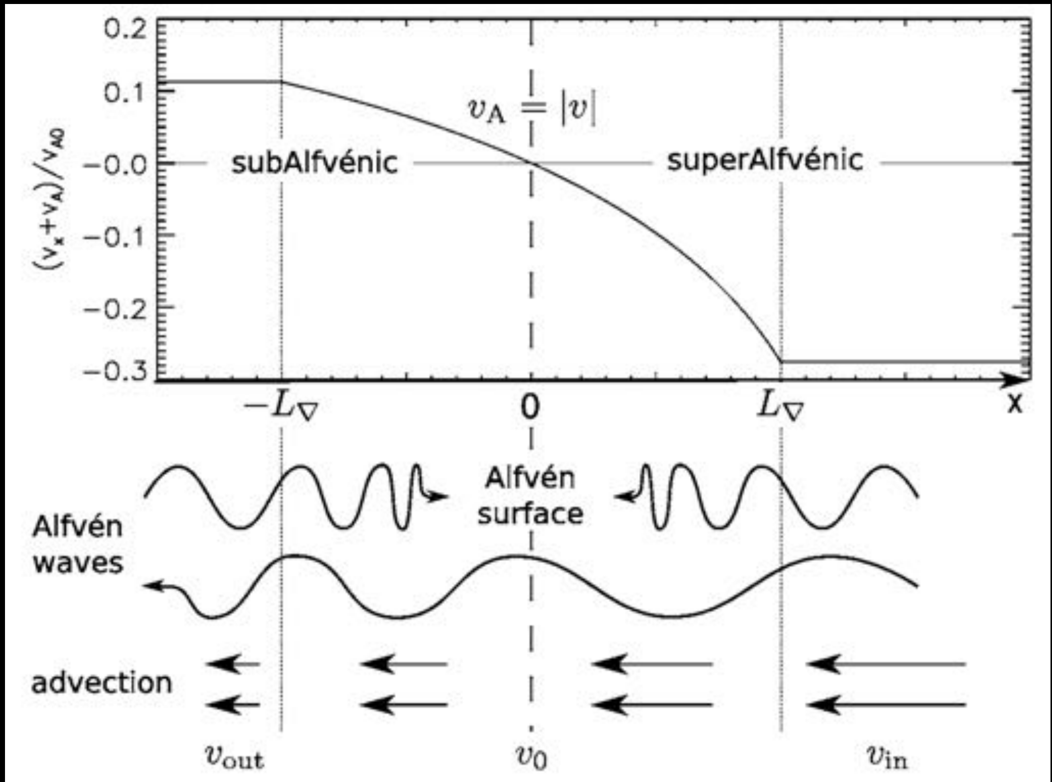

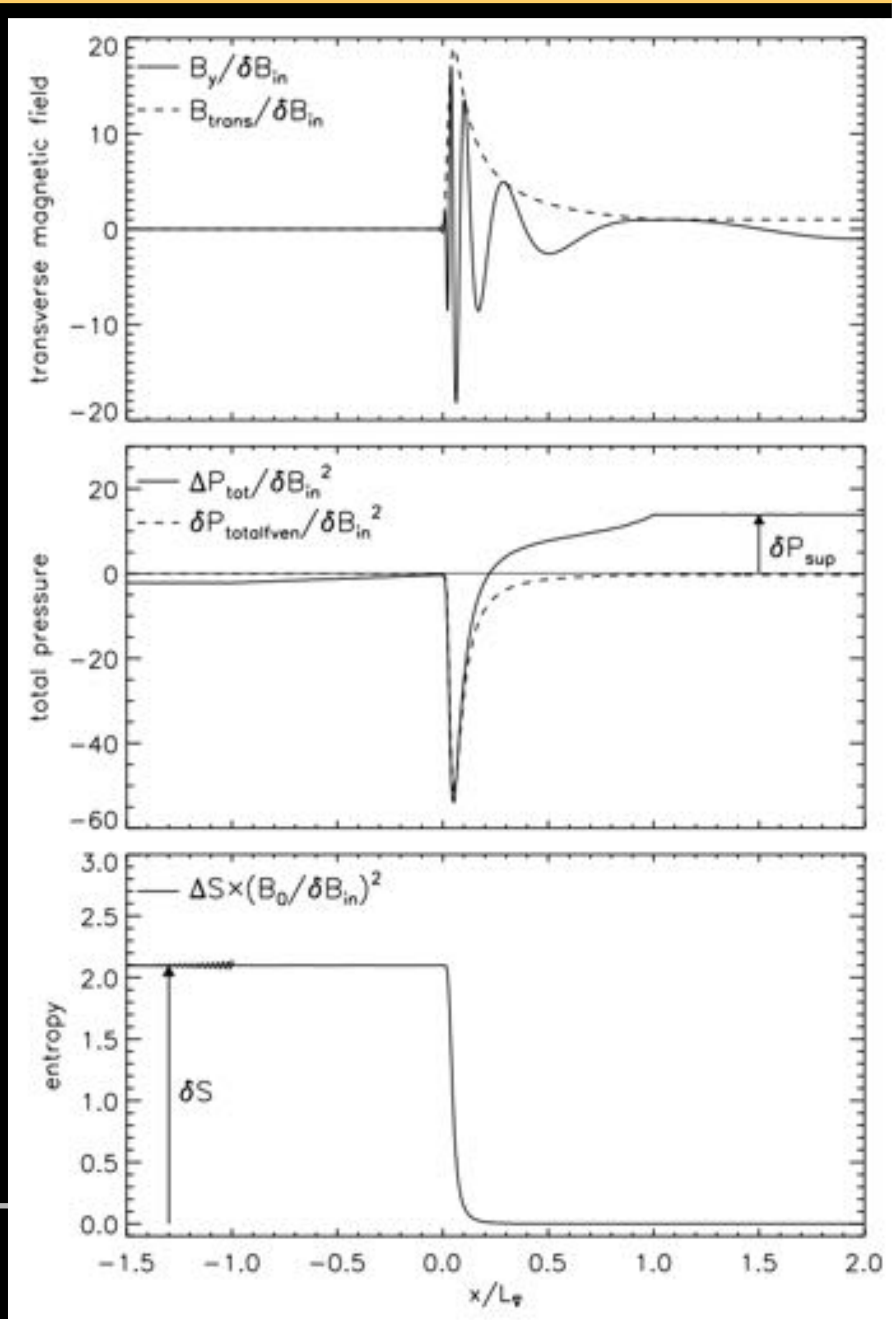

This effect has not been clearly identified in numerical simulations yet

Magnetic effects

Endeve+12

The turbulence induced by SASI is able to grow a significant magnetic field 10^{14}G at the surface of the protoneutron star, but with negligible consequences on the shock dynamics in 3D adiabatic simulations (Endeve+12), as well as in axisymmetric simulations of the full collapse unless the initial field strength is as large as 10^{12}G (Obergaulinger+14).

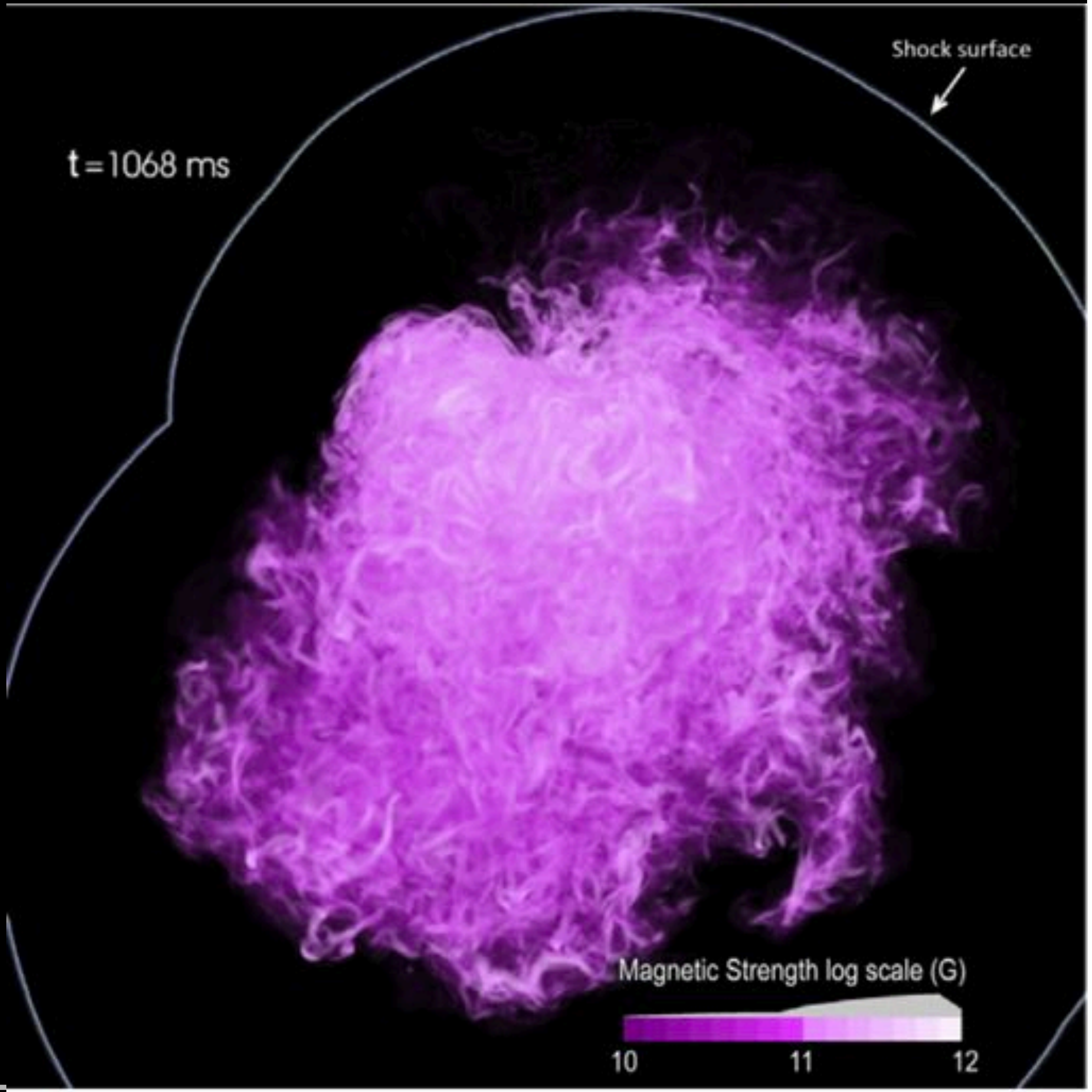

Magnetic effects with rotation: the magnetorotational instability

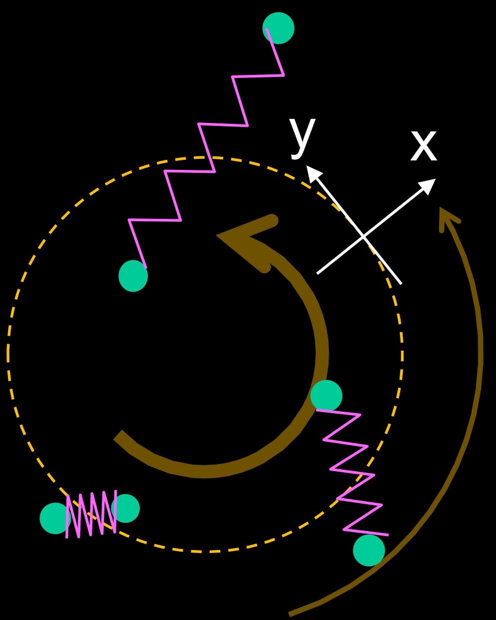

Differential rotation is able to amplify the magnetic field by connecting inner and outer orbits and acting as a restoring force (f_x, f_y)

The linearized system in the rotating frame is analogue to a particle attached with a spring to a guiding center

$$\frac{\partial^2 \xi_x}{\partial t^2} - 2\Omega \frac{\partial \xi_y}{\partial t} = -\frac{\partial \Omega^2}{\partial \ln R}\xi_x + f_x$$
$$\frac{\partial^2 \xi_y}{\partial t^2} + 2\Omega \frac{\partial \xi_x}{\partial t} = f_y$$

Hill equations

(Balbus & Hawley 92)

If B is along z, the restoring force is the magnetic tension in the direction perpendicular to the field, proportional to the Alfven speed V_A^2 associated to Alfven waves.

$$f_x = -(k_z V_A)^2 \xi_x$$
$$f_y = -(k_z V_A)^2 \xi_y$$

$$V_A \equiv \frac{B}{(4\pi\rho)^{\frac{1}{2}}}$$
$$V_c \equiv \frac{V_A c_s}{(V_A^2 + c_s^2)^{\frac{1}{2}}}$$

If B is along y, the spring is anisotropic: the restoring force f_y in the azimuthal direction is proportional to the cusp speed V_c^2 associated to slow magnetosonic waves (Foglizzo & Tagger 95)

$$f_x = -(k_y V_A)^2 \xi_x$$
$$f_y = -(k_y V_c)^2 \xi_y$$

Magnetic effects with rotation: the magnetorotational instability

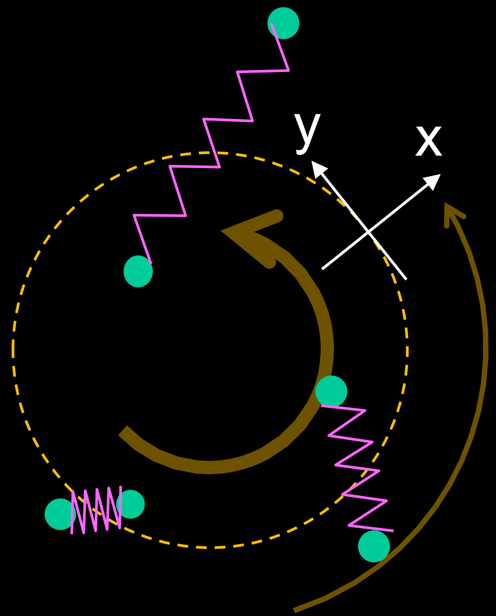

The dispersion of Alfven waves and slow magnetosonic waves modified by differential rotation is

$$\omega^4 - \omega^2 \left(\kappa^2 + k_z^2 V_{\rm A}^2\right) + k_z^2 V_{\rm A}^2 \left(k_z^2 V_{\rm A}^2 + \frac{\partial \Omega^2}{\partial \ln R}\right) = 0$$

where κ is the epicyclic frequency $\kappa^2 \equiv \frac{1}{R^3}\frac{\partial (R^2\Omega)^2}{\partial R}$

If the magnetic field is azimuthal, the dispersion relation involves both the Alfven speed and the sound speed.

$$\omega^4 - \omega^2 \left[\kappa^2 + \left(2 + \frac{V_{\rm A}^2}{c_{\rm s}^2}\right) k_y^2 V_{\rm c}^2\right] + k_y^2 V_{\rm c}^2 \left(k_y^2 V_{\rm A}^2 + \frac{\partial \Omega^2}{\partial \ln R}\right) = 0$$

The instability criterion is the decrease of the angular frequency, which destabilizes long wavelengths

$$(k \cdot V_{\rm A})^2 < -\frac{\partial \Omega^2}{\partial \ln R}$$

The maximum growth rate ω_{max} for a weak field is obtained for a wavelength λ_{max} proportional to the field strength B

$$\frac{2\pi V_{\rm A}}{\lambda_{\rm max}} \sim \Omega \left(-\frac{\partial \ln \Omega}{\partial \ln R}\right)^{\frac{1}{2}}$$

The growth of the magnetic field is possible until the magnetic tension stabilizes the longest available wavelength

$$\omega_{\rm max} = -\frac{1}{2}\frac{\partial \Omega}{\partial \ln R}$$

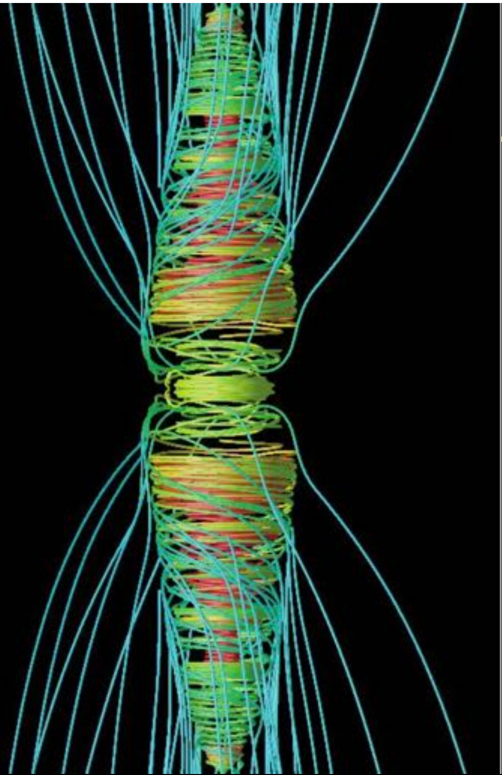

Burrows+07

Magnetic effects with rotation

$$\lambda_{\rm MRI}^{\rm max} \sim \frac{2\pi v_{\rm A}}{\Omega} \sim v_{\rm A} P \sim (10^4 \ {\rm cm}) P_{10} \frac{B_{12}}{\rho_{11}^{1/2}}$$

The small scale of this instability makes it very difficult to incorporate in numerical simulations of core collapse
→assumption of a large scale poloidal field in early 2D simulations (Burrows+07)

This amplification is affected by the neutrinos which diffuse momentum and act as viscosity for long MRI wavelengths, or a drag for the shortest ones (Guilet+15).

Stable stratification of entropy in the direction of the shear can stabilize the MRI (Guilet & Müller 15). Conversely, the MRI and the unstable stratification can both contribute to build up the magnetic field of a magnetar (ERC MagBurst, Guilet 17-22)

A strong jet can be formed in 3D (Mösta+15): a possible scenario for gamma ray bursts and superluminous supernovae

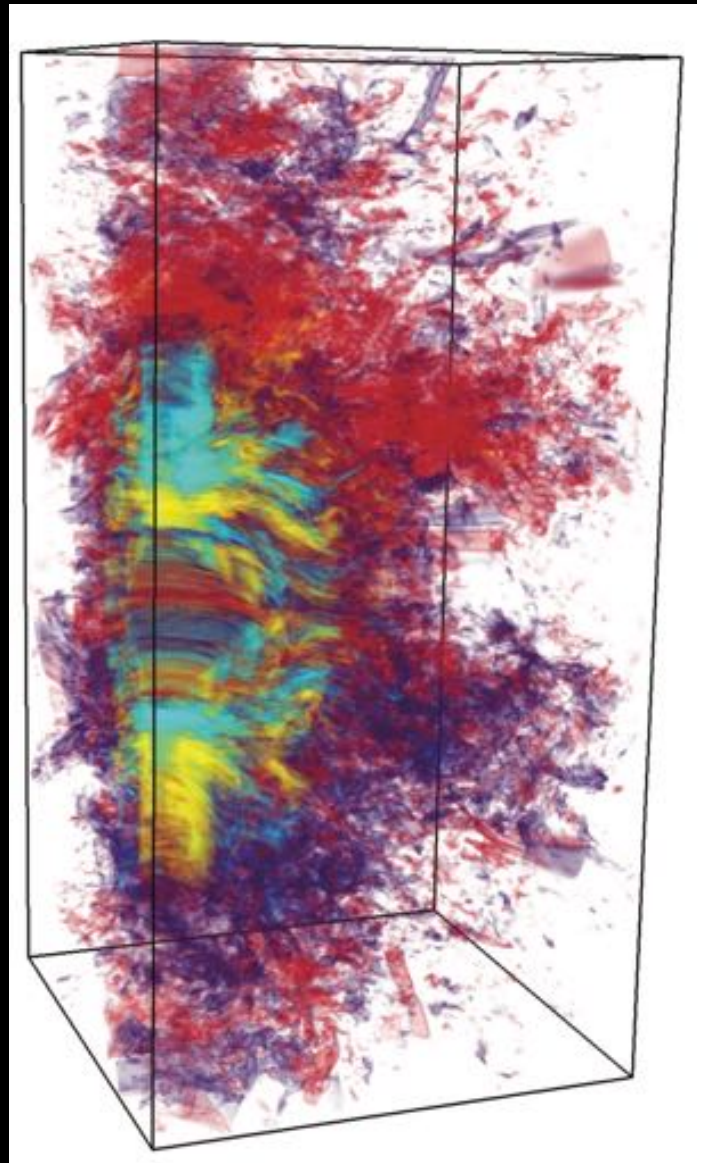

Mösta+15

Conclusion: 6 reasons to favour neutrino driven explosions

(adapted from Janka 13)

- 1- first principles & predicitive (no extreme or ad hoc ingredients)
- 2- successful explosion of low mass progenitors (8.8, 9.6M_{sol}) with Crab like properties
- 3- explosion can be successful in 2D
- 4- nucleosynthesis compatible: no overproduction of N=50 nuclei
- 5- NS kicks seem compatible with NS observations
- 6- SN mixing and asymmetries compatible with SN1987A

Conclusion

Hanke+13

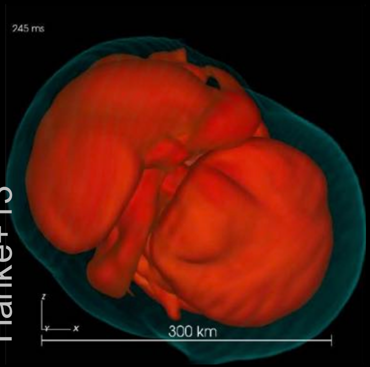

Recent progress in the theory core collapse supernovae benefited from

- -a larger scientific community
- -ab initio modelling in 2D→3D
- -the perspective of neutrinos and gravitational wave detection
- -progress in nuclear physics, EOS, microphysics
- -observations of SN progenitors, companions
  pulsars and black holes properties
  SNR composition, nucleosynthesis

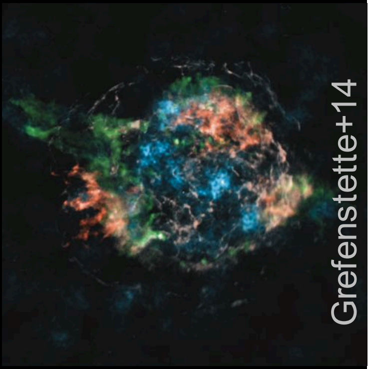

Grefenstette+14

LSST

Future progress will benefit from

- -improved SN and pulsar statistics with LSST, SKA
- -improved sensitivity of Advanced LIGO/VIRGO, HyperK
- -dedicated comparisons between numerical codes
- -improved modelling of stellar evolution
- -neutrino transport in 6+1D
- -observations of the direct collapse to a black hole
- -the explosion of a galactic supernova

HyperK

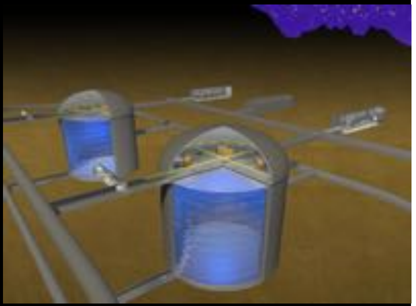

LIGO

SKA